

1 **Hydrothermal carbonization and liquefaction for sustainable production of**
2 **hydrochar and aromatics**

3 Yang Cao,^{a,b,c} Mingjing He,^c Shanta Dutta,^c Gang Luo,^{a,b} Shicheng Zhang,^{a,b} Daniel C.W.
4 Tsang^{c*}

5
6 ^a Shanghai Technical Service Platform for Pollution Control and Resource Utilization of
7 Organic Wastes, Shanghai Key Laboratory of Atmospheric Particle Pollution and Prevention
8 (LAP3), Department of Environmental Science and Engineering, Fudan University, Shanghai
9 200438, China.

10 ^b Shanghai Institute of Pollution Control and Ecological Security, Shanghai 200092, China.

11 ^c Department of Civil and Environmental Engineering, The Hong Kong Polytechnic University,
12 Hung Hom, Kowloon, Hong Kong, China.

13

14 *Corresponding author: E-mail: dan.tsang@polyu.edu.hk

15

Abstract

Sustainable biorefinery depends on the development of efficient processes to convert locally abundant, energy-rich renewable biomass into fuels, chemicals, and materials. Hydrothermal processing has emerged as an attractive approach for wet biomass conversion with less environmental burden. Although considerable efforts have been made in sustainable biorefinery by unitizing innovative technologies at a laboratory scale, its scaling-up is still impeded by the biomass heterogeneity. This article critically reviews the recent advances in hydrothermal carbonization and liquefaction technologies for the sustainable production of hydrochar and aromatics from different biomass wastes. Three main aspects, including lignocellulose-/lignin-rich feedstock, operating conditions, and design of liquid/solid catalysts, are critically reviewed and discussed to understand the reaction mechanisms and system designs for increasing the yields of aromatics and improving the properties of hydrochar. The latest knowledge and technological advances demonstrate the importance of identifying the physical and chemical properties of feedstock. The science-informed design of hydrothermal technology and optimization of operational parameters with reference to the biomass properties are crucial for the selective production of value-added chemicals and multifunctional hydrochar. This review identifies current limitations and offers original perspectives for advancing hydrothermal processing of biomass towards carbon-efficient resource utilization and circular economy in future applications.

Keywords

Biomass valorization; Lignocellulose; Sustainable biorefinery; Platform chemicals, Waste management; Engineered biochar/hydrochar.

40 **Abbreviation**

HTC: hydrothermal carbonization

HTL: hydrothermal liquefaction

HTG: hydrothermal gasification

GHG: greenhouse gas

HMF: hydroxymethylfurfural

HHV: higher heating value

H: *p*-hydroxyphenyl

G: guaiacyl

S: syringyl

*p*CA: *p*-coumarate

FA: ferulic acid

HDO: hydrodeoxygenation

XPS: X-ray photoelectron spectroscopy

FTIR: Fourier transform infrared spectrometer

NMR: nuclear magnetic resonance spectroscopy

LC-MS: liquid chromatography-mass spectrometry

GC-MS: gas chromatography-mass spectrometry

41

42 **1. Introduction**

43 Developing sustainable production of fuels, materials, and valuable chemicals from

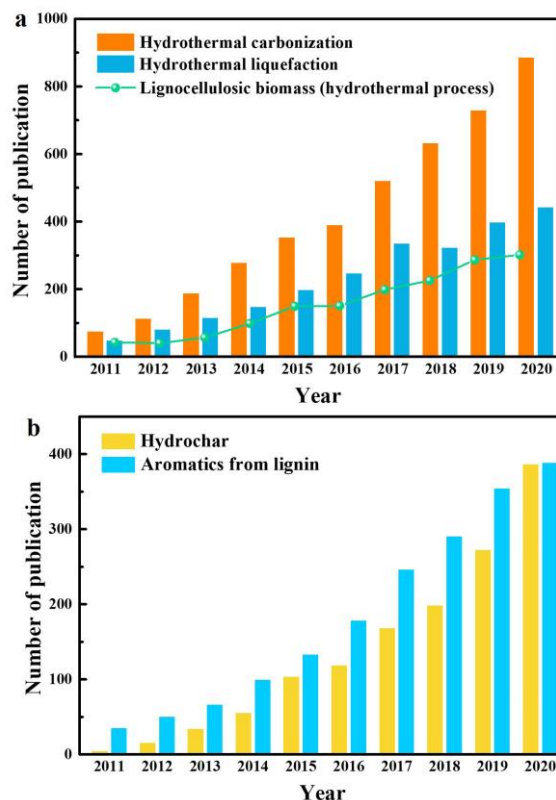
44 renewable feedstock have received considerable attention due to the rapid transition from fossil

45 fuel [1]. Biomass is a renewable organic material including wood, wood processing waste, yard
46 and garden waste, energy crop, algae, and municipal solid waste, etc. [2]. Lignocellulosic
47 biomass, such as woody waste and agricultural residues, is the most abundant resource with an
48 estimated annual global production of approximately 170 billion tons, and the utilization of
49 these renewable resources ensures a more sustainable society [3]. In terms of environmental
50 protection, using lignocellulosic biomass could effectively abate greenhouse gases (GHGs)
51 emissions, contributing to the mitigation of climate change by carbon sequestration [4].

52 Lignocellulosic biomass mainly consists of cellulose, hemicellulose, lignin, and extracts [5].
53 Most of the frontier biofuel production strategies focused on the conversion of hemicellulose
54 and cellulose [6, 7]. These precursors are the promising sources for producing lignocellulose-
55 derived sugars and valuable chemicals such as bioethanol, hydroxymethylfurfural (HMF),
56 furfural, and levulinic acid [8-12]. Nowadays, large amounts of lignocellulosic biomass are
57 processed in the pulp and paper industry which generates around 150-180 million tons of
58 technical lignin as industrial byproduct every year [13]. Lignin is one of the most abundant
59 sources of sustainable aromatics on the planet, but it is generally underutilized in these
60 cellulosic projects and mostly burned as fuel due to the challenges associated with its
61 recalcitrance and inherent heterogeneity [14, 15]. The variability of biomass composition
62 would result in products with different physicochemical properties and energy values. The
63 societal drive for a sustainable future highlights the recognition of lignin depolymerization into
64 aromatics (e.g., aromatic monomers, dimers, and low-molecular-weight oligomers), which
65 could improve the overall economic feasibility and sustainability metrics of biorefinery [16-
66 18]. To achieve sustainable production, not only the biomass feedstock but also the process

67 conditions should be carefully designed and tuned to obtain the desirable products.

68 Lignocellulosic biomass, though abundant in reserve for bioenergy production, has its own
69 drawbacks due to high moisture, bulk volume, and low heating value [19, 20]. Hydrothermal
70 processing is an effective and advanced technology that can directly convert carbon-rich
71 feedstock without prior drying step. This process is endothermic and usually carried out under
72 subcritical or supercritical water conditions, where the feedstock is fractionated into valuable
73 constituents through hydrolysis, depolymerization, and condensation [21]. Water is one of the
74 greenest solvents, and it can simultaneously act as a reactant and a suitable medium for acid-
75 catalyzed reactions to break down the biomass into small fractions by the high concentration
76 of H⁺ ions generated from subcritical water [21, 22]. Hydrothermal carbonization (HTC),
77 hydrothermal liquefaction (HTL), and hydrothermal gasification (HTG) are involved in the
78 processes for the selective production of carbonized solids (i.e., hydrochar), liquid bio-oils, and
79 fuel gases depending on the operating temperatures [23, 24]. HTC is conducted at temperatures
80 between 180 °C and 250 °C and produces hydrochar with properties similar to brown coal [25,
81 26]. The cellulose and hemicellulose fractions of lignocellulosic biomass can be largely
82 degraded into monomeric chains during the HTC process, whereas the lignin component is
83 mildly modified because of its recalcitrance. With increasing reaction temperatures, the lignin-
84 rich solid residues could be completely converted into liquid biofuel during the HTL process
85 at 250-370 °C and be gasified during the HTG process (370-750 °C) [27-29]. Thus, these routes
86 could realize various design of products with pre-defined properties and whole-biomass
87 valorization by an integrated process.



88

89 **Fig. 1.** Number of publications related to (a) hydrothermal technologies and (b) hydrochar
 90 and aromatics from 2011 to 2020 (according to Web of Science™).

91 By far, HTC and HTL have been particularly popular for the processing of biomass into
 92 value-added products at low to intermediate temperatures, *e.g.*, sustainable carbon-rich
 93 materials produced by HTC process, high selective production of aromatic monomers from
 94 HTL of lignin-rich feedstock, and novel catalytic approaches for HTL of algae towards biofuel
 95 production [30-33]. The number of publications related to hydrothermal processes between
 96 2011 and 2020 (according to Web of Science™) is shown in Fig. 1a. In particular, the interest
 97 in the production of hydrochar and aromatics has significantly increased because hydrochar
 98 can be a source of low-cost fuel energy replacing fossil fuels and lignin-rich feedstock offers
 99 significant valorization potential beyond its heating value for lignocellulose refining (Fig. 1b).
 100 Hydrothermal processing of lignocellulose-/lignin-rich feedstock presents an economically

101 attractive and environmentally friendly approach for sustainable biorefinery. However, several
102 fundamental and technical questions related to the variability in biomass, operating parameters,
103 and efficient catalysis need to be addressed in the hydrothermal processing of biomass into
104 desired products and commercialization of biofuels and bioproducts [34].

105 An overview of hydrothermal processing and its fundamentals as well as crucial issues of
106 hydrothermal conversion have been discussed above and reviewed in previous studies [23, 24,
107 31]. With regard to different hydrothermal routes, it is even more important to critically review
108 the advantages and challenges faced in the selective production of target products (*e.g.*,
109 hydrochar and aromatics), because the chemical conversion reactions and physical/chemical
110 challenges will differ when treating various types of biomass feedstock. HTC process is the
111 main subject of biorefinery research for producing solid hydrochar with different structures and
112 properties [35, 36]. The key factors including reaction temperature, time, pressure, loading ratio,
113 and use of catalyst can directly alter the reaction pathways and modify hydrochar for different
114 applications [20]. Hydrochar with a high energy density can be applied for energy storage while
115 it can also serve as a sustainable carbon material for environmental remediation and catalysis
116 [37-39]. HTL of lignin-rich feedstock can produce aromatic products with properties similar to
117 petroleum-derived counterparts. The influences of operating parameters on the selective
118 conversion of lignin have been widely studied to provide practical guidance, metrics, and
119 methods [40, 41]. Recent studies have highlighted that the selective production of targeted
120 aromatics would be determined by the inherent properties of lignin-rich feedstock [42-44].
121 Traditionally, most studies focus on the optimization of reaction parameters to tune the yields
122 and qualities of biofuel and bioproducts. Nevertheless, the critical impacts of feedstock

123 properties are often overlooked, which should be considered at the earliest stage to achieve
124 high-efficiency conversion. In-depth understanding with advanced analysis of feedstock
125 variability is essential for developing better production methods and understanding multiple
126 reaction mechanisms involved in the hydrothermal processes. In this case, extensive efforts are
127 still required to identify the correlations and interactions among feedstock properties and
128 targeted products.

129 We review the HTC of lignocellulose and HTL of lignin-rich feedstock for tailoring the
130 selective production of multifunctional hydrochar and aromatics with the aim to provide a
131 holistic and critical view on how the biomass variability, operational parameters, and catalyst
132 fundamentally affect its valorization. The key contributions of this work are to: (a) present the
133 important inherent properties of lignocellulosic biomass and physiochemical properties of their
134 derived hydrochar/aromatics; (b) evaluate the critical impacts of feedstock characteristics,
135 operating parameters, and use of catalysts on the yield and selective production of target
136 products; (c) illustrate the reaction mechanisms during the HTC and HTL processes when using
137 different lignocellulose-/lignin-rich feedstock with the optimized reaction parameters; (d)
138 identify the current limitations related to the scale-up of hydrothermal processes and provide
139 guidelines for sustainable biorefinery towards resource-efficient utilization in the future.

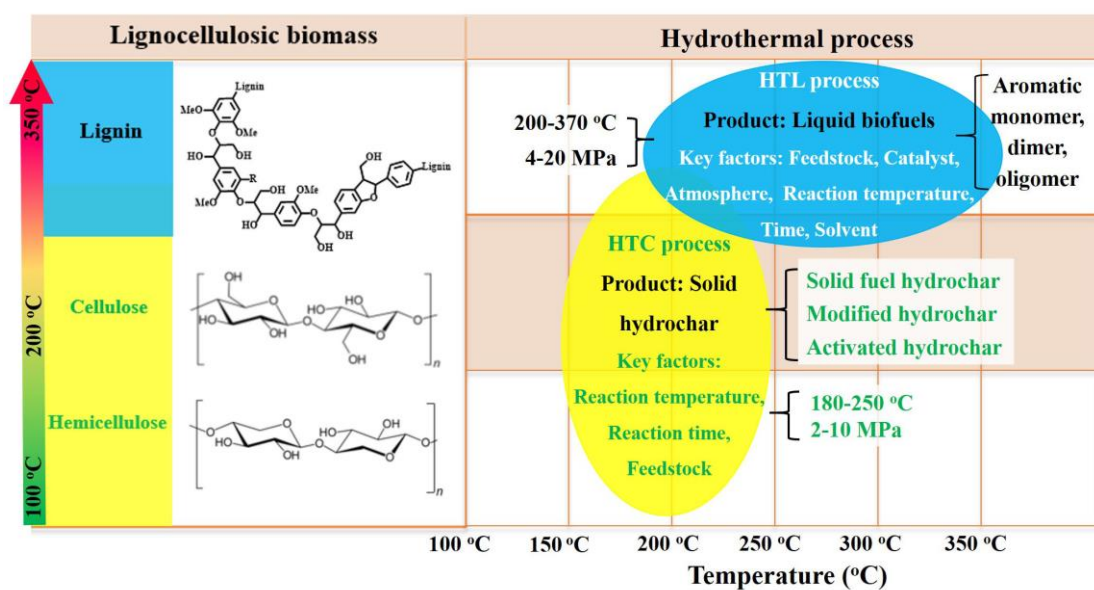
140 **2. Lignocellulosic biomass and hydrothermal process**

141 This section briefly summarizes the typical characteristics of lignocellulosic biomass and
142 key factors involved in HTC and HTL processes for the production of hydrochar and aromatics.

143 **2.1. Composition of lignocellulosic biomass**

144 Lignocellulosic biomass, such as grass, agricultural fibers, and wood-based residues, is a

145 promising alternative source for biorefinery due to its surplus availability and cost -
 146 effectiveness [45-47]. The major components of lignocellulosic biomass are cellulose,
 147 hemicellulose, lignin, and extractives (proteins and inorganic compounds) [5]. Cellulose is the
 148 most abundant polysaccharide in nature (making up 40-50% of dry weight of lignocellulose),
 149 mainly consisting of D-glucopyranose units linked by β -glycosidic bonds, as shown in **Fig. 2**
 150 [48, 49]. Hemicellulose is an amorphous biopolymer consisting of pentoses and hexoses other
 151 than glucose, accounting for 30-50% of lignocellulose [50, 51]. Lignin (10-30%) is an
 152 amorphous tridimensional polymer mainly composed of three types of building blocks: *p*-
 153 hydroxyphenyl (H), guaiacyl (G), and syringyl (S) units [52, 53]. These monolignols are linked
 154 through several types of C-O (e.g., β -O-4, α -O-4, and 4-O-5) and C-C (e.g., β - β , β -5, and 5-5)
 155 bonds during lignin biosynthesis [54]. In its native state, labile β -O-4 linkage is the most
 156 abundant and its cleavage shares the potential of producing aromatic monomer with a high
 157 yield. In addition, the extractives such as proteins and inorganic compounds are also present in
 158 small amounts [55].



160 **Fig. 2.** Structural formula of lignocellulosic biomass and key factors in hydrothermal processes.

161 Chemical composition analysis of various lignocelluloses is a tool to explain the feedstock
162 variability. Table 1 highlights the relative amounts of cellulose, hemicellulose, and lignin in
163 several typical lignocellulosic biomass [56-58]. Cellulose and hemicellulose are particularly
164 abundant in the grass biomass. Woody and nutshell wastes contain high contents of lignin that,
165 for example, makes up 43.9% of dry weight of walnut shell. Biomass variability results in
166 different chemical and physical properties, such as elemental compositions, higher heating
167 value (HHV), contents of fixed carbon and volatile matter. Downstream conversion needs to
168 consider these properties to take full advantage of biomass resources.

169

170 **Table 1.** Chemical compositions of the typical biomass [50-52].

Feedstock		Cellulose	Hemicellulose	Lignin
Hardwood	Poplar	42.1%	37.3%	24.8%
	Birch	41.7%	34.7%	21.9%
	Oak	40.4%	35.9%	24.1%
	Eucalyptus	39.0%	24.0%	29.0%
Softwood	Pine	42.1%	31.4%	20.4%
	Spruce	34.4%	29.8%	29.9%
Grass	Corn cob	33.3%	31.2%	16.2%
	Corn stover	51.2%	30.7%	14.4%
	Switchgrass	37.0%	26.0%	17.0%
Others	Endocarps	37.0%	25.4%	32.7%
	Almond shell	23.6%	27.6%	31.6%
	Walnut shell	13.4%	10.4%	43.9%

171 2.2. Hydrothermal carbonization for hydrochar production

172 Biomass typically contains a relatively high content of oxygen. It is an important object to
173 increase the energy density of biofuel by removing oxygen from biomass *via* dehydration or

174 decarboxylation reactions [59]. HTC is an environment-friendly technology to convert
 175 lignocellulosic biomass to solid biofuel. This process is typically conducted at low
 176 temperatures ranging from 180 °C to 250 °C and under 2-10 MPa, as shown in **Fig. 2**. Due to
 177 the high ionization of water, the acidic and basic nature of water can accelerate the
 178 carbonization process of biomass feedstock [21]. In general, substrates undergo hydrolysis,
 179 dehydration, decarboxylation, repolymerization, and condensation/aromatization in the HTC
 180 process [60, 61]. As a result, hydrochar with a high energy density can achieve comparable
 181 properties to brown coal. Moreover, HTC also provides hydrochar as a carbon-rich material
 182 with tunable structure through various controlled chemical processes. The advantages of HTC
 183 process are listed in **Table 2**. However, technological difficulties may be encountered during
 184 the reactions at a high solid loading rate, such as high energy consumption and rate-limiting
 185 heat and mass transfer.

186 **Table 2.** Advantages and disadvantages of different hydrothermal processes.

Process	Key Factors	Advantages	Disadvantages
HTC process	Feedstock; Operating parameters	Variable wet feedstock; Mild reaction condition; Multifunctional hydrochar	Low heat-transfer coefficient; Low selectivity; Multiple reaction pathways
HTL process (Lignin-rich feedstocks)	Lignin structure; Catalytic systems; Operating parameters	Moderate temperature; Selective production; Wide range of aromatic products	High pressure; Solid effect of feedstock; Uncontrolled condensation; Complex products

187 Many studies have established practices for hydrochar production and demonstrated that
 188 multiple types of feedstock, operation parameters, and subsequent modification or activation
 189 can alter hydrochar properties such as HHV, surface morphology, and textural structure [62,

190 63]. Typically, cellulose and hemicellulose undergo degradation at a considerably lower
191 temperature. The yields of hydrochar are lower at a higher reaction temperature due to the
192 enhanced hydrolysis and degradation of carbohydrate-rich feedstock with a larger amount of
193 small fragments dissolved in the liquid phase. In contrast, the decomposition of lignin-rich
194 feedstock into soluble products is hindered due to higher reaction temperature required [64].
195 Therefore, the hydrothermal reaction conditions should be selected based on the chemical
196 compositions of feedstock to obtain hydrochar with desired properties.

197 **2.3. Hydrothermal liquefaction for aromatics production**

198 Lignin is an irregular three-dimensional biopolymer that is hardly degraded during the HTC
199 process. With a higher temperature, the HTL process (200-370 °C, 4-20 MPa) can convert the
200 lignin-rich feedstock from the solid phase to valuable bio-oils such as aromatic monomer, dimer,
201 and oligomer (**Fig. 2**) [65, 66]. The lignin-rich feedstock in the high ionization of water is
202 subjected to hydrolysis and depolymerization *via* the selective cleavage of β -O-4 linkages into
203 small fragments in the presence of catalysts [67, 68]. Water properties differ at different
204 temperatures and influence the HTL process. Specifically, H^+ and OH^- derived from water
205 dissociation at high temperatures can act as the homogeneous acid/base catalysts, whereas the
206 solubility of solid substrate reduces due to the decrease in water density [21, 69]. Therefore,
207 the feedstock/water ratio should be optimized based on the dissolution capacity of water at
208 various reaction temperatures. Different from the key factors involved in HTC process (*e.g.*,
209 temperature and feedstock compositions), catalytic system is regarded as a key component
210 enabling lignin conversion in the HTL process, as listed in **Table 2**. Reductive and oxidative
211 approaches have been extensively studied for the selective production of desired products.

212 Moreover, catalytic systems with a high pressure of hydrogen or nitrogen can be explored to
213 further improve the production of aromatics. Nevertheless, the high-pressure requirement for
214 the HTL process may also present a major technical challenge for scaling up due to the safety
215 consideration and capital-intensive equipment requirement.

216 Various types of lignin feedstock (*e.g.*, wood, agro-waste, and technical lignin) have been
217 widely used for producing desired aromatic products. Initial structure of lignin varies and it
218 can govern the selective production of targeted aromatics. Native structure of lignin can be
219 altered easily by harsh pretreatments that cause the cleavage of β -O-4 linkages along with the
220 formation of stable C-C bonds, adding to the structural complexity of lignin [68]. Typically, the
221 modified lignin through extraction or pretreatment exhibited a limited yield of aromatics
222 because the depolymerization and condensation of lignin fragments are concomitant. To
223 achieve efficient valorization of lignin-rich feedstock, it is essential to improve the lignin
224 quality with less complexity and prevent its repolymerization and formation of recalcitrant
225 structures. Furthermore, understanding the mechanisms of depolymerization and condensation
226 of lignin-derived intermediates is an effective strategy towards aromatics production with a
227 higher yield.

228 **3. Hydrothermal carbonization**

229 **3.1. Biomass feedstock**

230 Feedstock plays a significant role in the product yield, surface functional groups, textural
231 structure, chemical composition, and surface morphology of hydrochar. The effects of
232 feedstock on producing multifunctional hydrochar are reviewed in **Table 3**. The high content
233 of lignin typically leads to an increase in the yield and thermal stability of hydrochar [70, 71].

234 Hydrochar derived from carbohydrate-rich feedstock has abundant hydroxyl groups and
235 enrichment of aromatic carbons [71]. Previous studies compared the differences in the yield
236 and redox capacity among Zn-loaded lignin-, cellulose-, and D-xylose-derived hydrochar. The
237 addition of Zn(II) could increase the redox capacity of lignin-derived hydrochar due to the
238 presence of phenolic hydroxyl and surface active -COOH groups [72]. These functional groups
239 are the essential active sites for wastewater treatment by adsorption/degradation of various
240 pollutants. The hydrochar surface properties are correlated to the compositions of biomass
241 feedstock. Hydrochar produced from spruce sawdust and wheat were more acidic than those
242 produced from canola straw and non-lignocellulosic feedstock [73]. The CO₂ released from
243 lignocellulosic biomass could form carbonic acid, resulting in an acidic condition during HTC
244 process. The depolymerization of lignin-rich feedstock could produce abundant phenol-derived
245 products, which may also affect the acidity of hydrochar.

246 Pretreatment of raw feedstock also impact the hydrochar properties. Intensive grinding of
247 feedstock is an effective strategy to increase the specific surface area of the resultant hydrochar,
248 and subsequent activation can produce a potential carbon material for high-performance
249 supercapacitor [62]. HTC of corn stalk before and after anaerobic digestion were employed to
250 investigate the influence of pretreatment on the quality of solid fuel [74]. The results showed
251 that anaerobic digestion activated amorphous cellulose and increased the carbon content and
252 HHV of produced hydrochar, whereas the content of mineral constituents decreased due to
253 leaching in anaerobic digestion.

254 In the HTC process, cellulose, glucose, fructose, and lignin extracts, etc., could be used to
255 produce spherical carbon-based materials by self-assembly [75-78]. The specific structures of

256 hydrochar have been applied in the preparation of catalysts or high-performance carbon-rich
 257 materials for water purification and energy storage. HTC of enzymatic lignin at 160 °C for 12
 258 h produced highly regular spherical aggregates *via* π - π interaction of lignin fragments [76],
 259 while higher reaction temperature promoted the cleavage of β -O-4 linkages and dehydration
 260 reaction, resulting in a decreased content of carboxyl groups. Wang et al. [79] reported glucose
 261 as a promising carbon source that can be used to prepare hollow carbonaceous materials with
 262 abundant active sites, which showed a superior electrochemical performance. Zhang et al. [80]
 263 used fructose as a carbon source for the preparation of mesoporous support by using P123 and
 264 F127 as soft templates through a hydrothermal reaction at 180 °C for 24 h. Its high specific
 265 surface area contributed to the high dispersion of Ru-based catalysts with porous structures.
 266 Overall, the starting feedstock is of significance for selectively producing the targeted carbon
 267 materials with specific structures and functionalities via the HTC process.

268 **Table 3.** Effects of feedstock selection and process conditions on HTC process.

Feedstock	Conditions	Key Findings	Ref.
Sunflower stalk	230 °C, 24 h, 2/40 (w/v)	Grinding of feedstock (8000 mesh) contributed to an obvious increase in specific surface area of the hydrochar (720 m ² /g). This material was further activated by KOH to increase its surface area (1505 m ² /g), and showed high electrochemical storage capacity for high-performance supercapacitor.	[62]
Wood	220 °C, 1 h; 20/80 (w/v)	Lignin-rich woody biomass was used to produce activated carbon for adsorption <i>via</i> the HTC process and two-step chemical activation with KOH. The functional groups, surface area, and pore size distribution are strongly related to the HTL process and feedstock.	[70]
Canola straw, Wheat straw, Sawdust	180-300 °C, 1/8 (w/v)	Feedstock type (lignocellulosic and non-lignocellulosic feedstock) and HTC temperature affected the elemental compositions and biofuel properties of hydrochar. The hydrochar from lignocellulosic biomass at 240 and 300 °C had a low content of ash and resembled high-volatile bituminous coal.	[73]

Lignin	300-390 °C	The low surface area of lignin-derived hydrochar was activated with KOH to yield carbon-based material with a high surface area of 3235 m ² /g and pore volume of 1.77 cm ³ /g, which displayed a good hydrogen uptake of 6.2 wt% at -196 °C and 2 MPa.	[77]
Kraft lignin	240 °C, 22 h, H ₂ SO ₄ /FeCl ₂ , 10/100 (w/w)	Homogeneous acid catalyst (H ₂ SO ₄) promoted the degradation of lignin-rich biomass through the cleavage of carbon side chains and β-O-4 linkages, resulting in a higher yield of solid hydrochar with a more stable structure.	[64]
Lignin, Cellulose, D-xylose,	240 °C, 4 h, ZnSO ₄ , 10/50 (w/v)	The hydrochar yields from cellulose, D-xylose, and lignin showed an increased trend with the values of 33.9%, 36.0%, and 45.3%, respectively. Zn(II) catalyst significantly altered the redox capacity of lignin-derived hydrochar by inhibiting the decomposition of phenolic hydroxyl group, which could be used for reductive degradation of toxic organics.	[72]
Cellulose	200 °C, 48 h, Al(OTf) ₃ , 1.5/20 (w/v)	Acidic Al(OTf) ₃ catalyst promoted the degradation of cellulose, and its derived hydrochar showed a spherical morphology with a diameter of 300-600 nm.	[78]
Glucose	180 °C, 8 h, 8/80 (w/v)	HTC of glucose produced uniform carbon nanospheres, which were then calcined under NH ₃ atmosphere and activated by CO ₂ to form N-doped carbon nanospheres with high specific surface area (2813 m ² /g) for electrocatalytic oxygen reduction.	[75]
Fructose	180 °C, 24 h, 2/70 (w/v)	The mesoporous carbon supports were prepared by using P123 and F127 as the composite templates and fructose as the carbon source <i>via</i> HTC process. High specific surface area of carbon-based support provided abundant active sites for heterogeneous catalysis.	[80]

269 3.2. Operating conditions

270 3.2.1. Reaction temperature

271 HTC temperature is a critical factor that directly affects the hydrolysis of biomass feedstock
272 as well as the degradation and carbonization of newly formed intermediates for the production
273 of hydrochar. In general, a gradual increase in C content and a corresponding loss of H and O
274 contents occurred when increasing the reaction temperature through the enhanced
275 deoxygenation and dehydration reactions, as shown in **Table 4** [25, 26, 81]. For instance,
276 Cuevas et al. [58] investigated the short-time HTC of olive endocarps to identify the hydrochar

277 properties with different reaction temperatures. High HTC temperatures would facilitate free
 278 radical generation and promote biomass degradation, whereas the yield of hydrochar decreased.
 279 Keiller et al. [82] employed 200 °C, 230 °C, and 260 °C to investigate the changes in functional
 280 groups and compositions of hydrochar from saltbush. At 260 °C, the decarboxylation reaction
 281 of cellulose resulted in the loss of C=O carbonyl groups and the formation of formic acid and
 282 CO₂. The contents of hemicellulose, cellulose, and lignin in Saltbush declined from 21%, 24%,
 283 and 28% to 0%, 6%, and 17%, respectively. These results confirmed that the high temperature
 284 could effectively promote the degradation of carbohydrate-rich feedstock. By contrast, lignin
 285 only partly hydrolyzed and a large proportion of insoluble lignin remained in hydrochar. HTC
 286 of raw food waste (76% moisture content), containing vegetables, fruits, and staple food,
 287 resulted in a low yield of hydrochar with only 7% at 200 °C and 5% at 300 °C [83]. The yields
 288 of hydrochar from dried food waste ranged 44-53.1% at 160-200 °C for 5 h, with an energy
 289 densification of 5.5-7.3 [84].

290 **Table 4.** Characterization of various biomasses and their derived hydrochar.

Feedstock	Conditions	C	H	O	FC	Ash	HHV	Yield	Ref.
Endocarps	Raw	49.65	6.83	42.68	13.06	0.71	18.78	-	[58]
	175 °C, 0-10 min	49.12	6.73	43.73	13.32	0.28	20.50	97	[58]
	200 °C, 0-10 min	49.34	6.67	43.64	14.22	0.21	20.88	85	[58]
	225 °C, 0-10 min	51.77	6.68	41.26	18.23	0.2	21.90	61	[58]
Corn cob	Raw	43.1	5.8	44.6	17.2	4.2	17.2	-	[58]
	190 °C, 1.5 h	46.7	5.5	43.9	19.2	3.7	18.1	66	[81]
	250 °C, 1.5 h	65.0	4.6	24.5	44.3	6.4	25.5	45	[81]
	310 °C, 1.5 h	67.7	4.5	20.9	51.6	6.3	26.6	38	[81]
	370 °C, 1.5 h	70.3	4.3	17.8	65.8	7.0	27.6	33	[81]
Corn stover	Raw	45.12	5.77	45.19	17.15	3.51	17.8	-	[25]
	180 °C, 4 h	48.05	5.34	43.85	19.57	2.40	18.4	68	[25]
	200 °C, 4 h	50.10	5.26	43.85	24.18	2.38	19.1	62	[25]
	220 °C, 4 h	62.64	5.21	28.95	38.75	2.79	24.9	51	[25]

	220 °C, 2 h	61.21	5.22	30.61	29.62	2.58	24.3	56	[25]
	220 °C, 12 h	67.36	5.01	24.26	49.78	2.97	26.8	50	[25]
Mallow	Raw	44.9	6.02	46.78	5.62	1.97	17.8	-	[25]
	180 °C, 1 h	49.7	5.77	42.72	9.75	1.40	19.7	66	[26]
	200 °C, 1 h	52.5	5.78	40.21	14.42	1.05	20.9	61	[26]
	220 °C, 1 h	54.5	5.67	38.39	16.04	1.05	21.7	56	[26]
Canola straw	Raw	48.6	4.9	39.9	2.6	5.6	18.5		[73]
	180 °C, 4 h	53.2	5.2	32.9	10.8	8.1	21.2	61	[73]
	240 °C, 4 h	68.1	5.5	18.5	11.7	5.6	28.2	43	[73]
	300 °C, 4 h	72.0	5.1	13.9	30.3	7.2	29.6	26	[73]
Olive tree	Raw	49.98	6.45	37.67	26.6	3.86	21.2		[85]
	200 °C, 1 h	55.43	6.15	29.78	31.99	6.59	23.4	82	[85]
	250 °C, 1 h	60.29	5.87	23.41	38.63	7.97	25.4	66	[85]
	300 °C, 1 h	63.39	5.01	18.58	56.74	9.97	26.0	51	[85]
	350 °C, 1 h	64.40	5.02	15.88	64.71	11.95	26.5	39	[85]
Vineyard	Raw	47.14	6.46	43.25	30.2	2.0	23.9		[85]
	200 °C, 1 h	51.86	5.77	38.50	32.19	3.09	20.9	82	[85]
	250 °C, 1 h	58.78	5.28	30.81	43.39	3.62	23.5	63	[85]
	300 °C, 1 h	65.78	4.22	23.05	67.85	5.37	25.4	42	[85]
	350 °C, 1 h	72.35	4.03	13.99	73.22	7.91	28.4	37	[85]
Food waste	Raw	39.00	7.32	47.68	14.48	6.41	15.0		[83]
(76%	200 °C, 1 h	62.83	7.25	24.88	30.34	4.52	20.81	7	[83]
moisture)	250 °C, 1 h	68.10	7.09	20.09	45.41	3.11	28.89	6	[83]
	300 °C, 1 h	73.00	7.01	17.09	47.43	2.21	31.00	5	[83]
Food waste	Raw	52.0	6.9	38.1	5.0	1.8	15.1		[84]
(dried)	160 °C, 5 h	51.5	7.0	31.1	1.7	5.9	23.3	52	[84]
	180 °C, 5 h	61.4	6.6	24.6	2	0.9	29.5	44	[84]

291 Raw: biomass feedstock; Weight content of O was calculated by difference ($O\% = 100\% - \text{ash}\%$
292 $- C\% - H\% - N\% - S\%$).

293 3.2.2. Reaction time

294 Reaction time also influences the chemical, morphological, and structural properties of
295 hydrochar. Prolonged reaction time could result in continuous hydrolysis and simultaneous
296 polymerization of degraded fragments, forming the secondary char with a complex structure.

297 The increases in HHV and content of fixed carbon due to the removal of oxygen from biomass
298 feedstock are listed in **Table 4** [26, 58, 81]. Johnson et al. [86] found that the yields of hydrochar
299 decreased from 55% to 35% from 3 h to 7 h while the HHV value steadily increased from
300 200 °C (11.4 MJ/Kg) and approximately doubled at 250 °C (24.9 MJ/Kg). Zhang et al. [25]
301 revealed that a longer reaction time resulted in the decrease of hydrochar yields and H/C (0.76-
302 1.33) and O/C (0.19-0.68) ratios due to the dehydration and decarboxylation reactions.
303 Regarding the effects of time on morphological properties of hydrochar, increasing the reaction
304 time from 4 h to 24 h could strongly destruct the initial structure of corn stover and accelerate
305 the formation of nanospheres and microfiber at high reaction severity. Similar results were
306 reported by Zhang et al. [63], in which the long reaction time obviously destroyed the fiber
307 structure of wheat straw and produced carbon microspheres after HTC process.

308 **3.3. Catalyst**

309 Various catalysts were explored to develop the multifunctional hydrochar materials by a
310 controlled chemical process. In general, the modification using acids such as H₂SO₄, H₃PO₄,
311 and organic acids facilitated the establishment of high surface area and porous structure of
312 hydrochar [87, 88]. Acid-assisted HTC was conducted to produce functionalized carbon-based
313 catalysts [87], in which Kraft lignin feedstock was carbonized and sulfonated with the H₂SO₄
314 catalyst at 180 °C for 12 h. An increase in acidic groups over the surface of lignin-derived
315 hydrochar catalyst was detected, and these oxygenated groups were supposed as the active sites
316 to promote the dehydration of fructose. Xu et al. [88] reported that acids could drive the self-
317 assembly of F127 micelles and pentose into the stable structure and contributed to the
318 formation of hydrochar at a low temperature. The hydrochar yield is also affected by the

319 promoted hydrolysis of feedstock with acidic catalyst. Simsir et al. [78] reported that the yields
320 of hydrochar from both cellulose and glucose were reduced by the addition of acidic $\text{Al}(\text{OTf})_3$
321 catalyst, while the yield increased in the presence of alkaline catalysts because of the inhibition
322 of secondary char formation.

323 Biomass loaded with different concentrations of metal salts (Fe^{3+} , Ni^{2+} , Cu^{2+} , or Zn^{2+}) have
324 also been explored to modify the surface and structure of hydrochar for pollutant degradation,
325 catalysis, and energy storage [89, 90]. Zhu et al. [91] activated the forestry waste by zinc
326 chloride (ZnCl_2) for producing hydrochar with a high porosity. The condensation of aromatics
327 and removal of tar were promoted in the presence of ZnCl_2 catalyst, and the addition of K_2CO_3
328 further broadened microporosity distribution of the resultant hydrochar. The promotional effect
329 of Zn^{2+} on surface groups was investigated by Ma et al. [72], who found the decline in carboxyl
330 groups and the increase in phenolic hydroxyl groups in the Zn-loaded hydrochar. The difference
331 was attributed to metal adsorption that hindered the subsequent dehydration reaction of
332 phenolic hydroxyl groups. Li et al. [92] reported richer oxygenated groups, higher carbon
333 content (up to 64%), and improved specific surface area, average pore size, and pore volume
334 by subsequent HCl washing that removed ZnCl_2 from the channels of Zn-modified bamboo
335 hydrochar. Xu et al. [93] similarly improved the porosity of bamboo hydrochar by the addition
336 of $\text{Fe}_2(\text{SO}_4)_3$ in the HTC process while retaining the spherical morphology. The Fe-decorated
337 carbon sphere could be a potential electrode material for high-performance supercapacitor
338 application. In addition, mineral ash as catalysts play an important role in the yield and quality
339 of hydrochar [94, 95]. The yield of hydrochar derived from *Scenedesmus* with a high ash
340 content is lower than that from the de-ashed feedstock, indicative of the catalytic hydrolysis of

341 biomass due to ash content [95]. Nevertheless, feedstock de-ashing by acid washing could
342 enrich the carbon content and enhance the quality of hydrochar as a solid fuel.

343 **3.4. Reaction pathway**

344 Reaction pathways in the HTC process can be categorized into three steps: hydrolysis,
345 decomposition, and carbonization/polymerization of degraded products, as shown in **Fig. 3**
346 [96-98]. Firstly, lignocellulosic biomass is hydrolyzed to small soluble fragments and key
347 intermediates in the liquid phase. The solution pH value decreases due to the formation of
348 organic acids and phenolic chemicals. Secondly, the degraded fragments, including monomers
349 (*e.g.*, glucose, xylose, 5-HMF, furfural, and their derived products) and oligomers undergo
350 dehydration and polymerization, and the insoluble phase precipitates slowly from the liquid
351 phase. As a result, the hydrochar is formed through the final step of aromatization reaction
352 along with decarboxylation reaction. This process is adequate for hemicellulose, cellulose, and
353 soluble lignin. The predominant mechanism differs when using different types of feedstock
354 that contain variable contents of cellulose, hemicellulose, and lignin. For instance,
355 hemicellulose-rich feedstock has a low degree of polymerization as compared to cellulose and
356 lignin-rich feedstock. At low temperatures, hydrolysis of hemicellulose mainly generates xylo-
357 oligomers. When increasing the reaction temperature up to 180 °C, monomeric xylose and
358 furfural resulting from dehydration of pentoses were the key intermediates accountable for the
359 formation of insoluble secondary char through the polymerization reaction.

HTC process

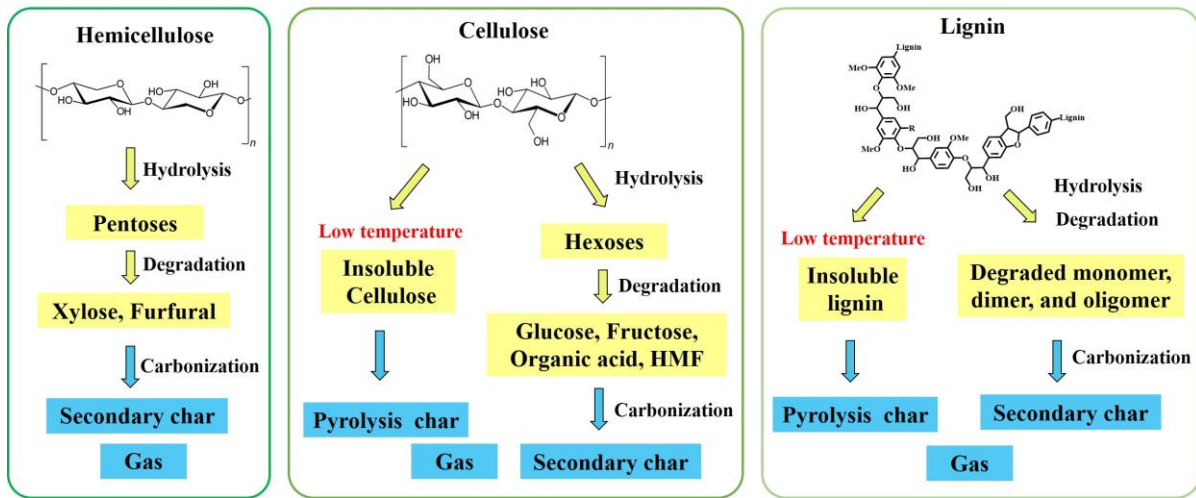
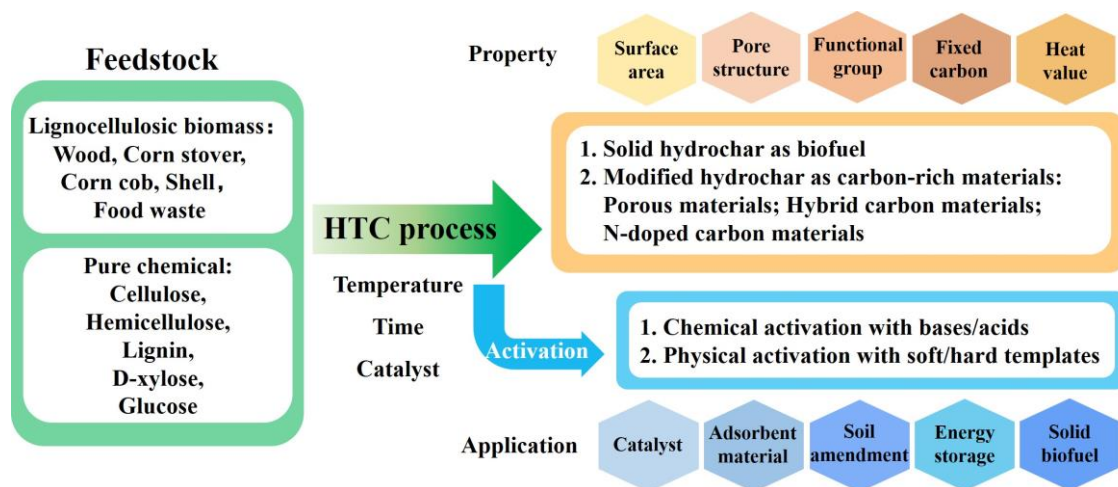


Fig. 3. Reaction pathways of HTC process.

The mechanisms proposed for HTC processing of cellulose-rich and lignin-rich feedstock include two pathways, *i.e.*, soluble pathway and insoluble pathway, which depend on the reaction temperature. In general, cellulose can be degraded into soluble fragments above 200 °C, while it is partly subjected to hydrolysis at a low temperature [99]. The soluble products (*e.g.*, glucose oligomers, glucose, and fructose) from cellulose subsequently undergo a series of reactions, including isomerization, dehydration, and fragmentation into active intermediates such as HMF and organic acids. These reactive products can be polymerized and condensed to form the secondary char. The insoluble parts are subjected to a pyrolysis-like reaction at a low reaction temperature [99]. As lignin is an amorphous heteropolymer with a low solubility in water, the hydrolysis of lignin into soluble fragments (*e.g.*, aromatic monomer, dimer and oligomer) is the critical limiting factor for the formation of secondary char [64]. The majority of insoluble lignin are subjected to mild dehydration and decarboxylation reactions and then remain as the pyrolysis char [72], as shown in **Fig. 3**.

3.5. Properties and applications of hydrochar

376 The key characteristics and possible applications of multifunctional hydrochar from HTC of
 377 various feedstock are illustrated in **Fig. 4**. The proximate and ultimate analysis of hydrochar is
 378 necessary to ensure an efficient utilization of hydrochar as a solid biofuel. The proximate
 379 analysis includes volatile matter, ash, and fixed carbon. The O/C and H/C ratios, as well as
 380 yields of hydrochar, can illustrate the degree of carbonization of biomass feedstock with
 381 variable reaction severities. Typically, Van Krevelen diagram that is used to illustrate the H/C
 382 and O/C ratios can indicate the degree of dehydration and decarboxylation reactions and
 383 provide a direct comparison between raw feedstock and its derived hydrochar [100, 101], which
 384 is exemplified in **Fig. 5a**. The HHV is directly related to the contents of C, O, N, S, and ash
 385 [60]. Increasing reaction severity usually results in a higher percentage of fixed carbon and a
 386 decrease in the contents of ash and O, thus improving the HHV of hydrochar.



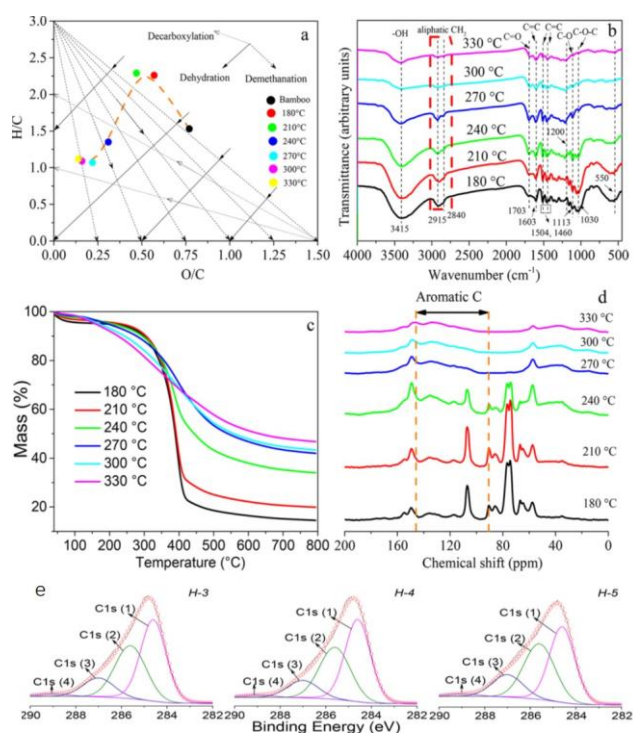
387

388 **Fig. 4.** HTC of various feedstock to produce multifunctional hydrochar.

389

390 Advanced structure analysis enables a comprehensive understanding of hydrochar properties
 391 after different treatments. The physicochemical changes are often assayed by using FTIR,
 392 NMR, and XPS (**Fig. 5b-e**) [102-104]. FTIR is widely used to identify the surface functional

393 groups (e.g., C=C bonds, -OCH₃, and -OH groups) and reveal the evolution of structural
 394 characteristics under different HTC conditions [105]. NMR is employed to provide valuable
 395 quantitative data for surface functionality analysis [106], and 2D NMR provides detailed
 396 information about the intermolecular linkages and aromatic structures existing in the complex
 397 lignin feedstock [107, 108]. XPS reveals the chemical environment of hydrochar surface. Two
 398 prominent peaks in C (C1s) and O (O1s) are usually investigated in XPS spectra to determine
 399 the functional groups on the hydrochar surface [109]. The surface morphology and textural
 400 properties of hydrochar are significantly affected by biomass feedstock and carbonization
 401 temperature. The morphology changes and structural evolutions are generally evaluated by
 402 SEM and BET analyses for the specific surface area and pore size distribution. The above
 403 physicochemical properties provide fundamental information of the material characteristics for
 404 the rational design of the multi-functionality of hydrochar.



405
 406 **Fig. 5.** (a) H/C and O/C atomic ratios in Van Krevelen diagram, (b) FTIR spectra, (c)

407 thermograms, (d) solid-state ^{13}C NMR spectra, and (e) XPS spectra of hydrochar [100, 101].

408 However, the low surface area and underdeveloped porosity of hydrochar may hinder its
409 diverse utilization. To address this limitation, a range of strategies have been investigated for
410 improving its physicochemical properties and morphologies, such as the incorporation of
411 heteroatom, hierarchical porosity customization, and introduction of surface defects to expand
412 their applications [110-112]. For example, a two-stage HTC and chemical activation
413 technology method was applied to prepare activated hydrochar with large surface areas and
414 enriched pore structures [113]. Chemical activation with acids, bases, and metal salts was
415 explored to increase the surface area and porosity of hydrochar. Activation using KOH was
416 conducive to establishing pore structures, exposing more active sites and oxygen-containing
417 functional groups, and boosting the potential application of hydrochar in energy storage,
418 pollutant adsorption, and catalysis, as listed in **Table 5**. For instance, activation of lignin-
419 derived hydrochar by KOH could generate carbon-based materials with a high surface area up
420 to $3235\text{ m}^2/\text{g}$ that served as a superior sorbent for hydrogen storage [77]. The high content of
421 undegraded lignin made hydrochar richer in oxygenated functional groups that could be the
422 active sites for pollutant adsorption and degradation [70].

423 Furthermore, physical activation by using CO_2 or the use of soft template can effectively
424 enlarge the pore size of hydrochar [75, 114]. The CO_2 activation of hydrochar can also
425 significantly increase the specific surface area due to the carbon loss by incomplete
426 carbonization process ($\text{C} + \text{CO}_2 \rightarrow 2\text{CO}$) [75]. In the latest studies, heteroatom doping has
427 been a major research subject to improve the physiochemical properties of hydrochar [115].
428 Nitrogen-doped carbon materials showed a remarkable performance in many applications such

429 as pollutant adsorption, gas storage/separation, and catalytic reaction [39, 115]. The blending
 430 of lignocellulosic biomass with nitrogen-rich materials (*e.g.*, protein, urea, Spirulina) in the
 431 HTC process can effectively improve the nitrogen doping level and introduce structural
 432 nitrogen into the resultant hydrochar [111, 112]. Besides, food waste and yard waste could be
 433 mixed in the HTC process for the solid biofuel production, and the HHV increased to 27.6
 434 MJ/kg at 220 °C for 1 h [116]. Microwave-assisted HTC of corn stalk at 230 °C also produced
 435 solid biofuel with a high energy density [117]. Overall, modification/activation approaches are
 436 critical to improve the performance of hydrochar-based carbon materials.

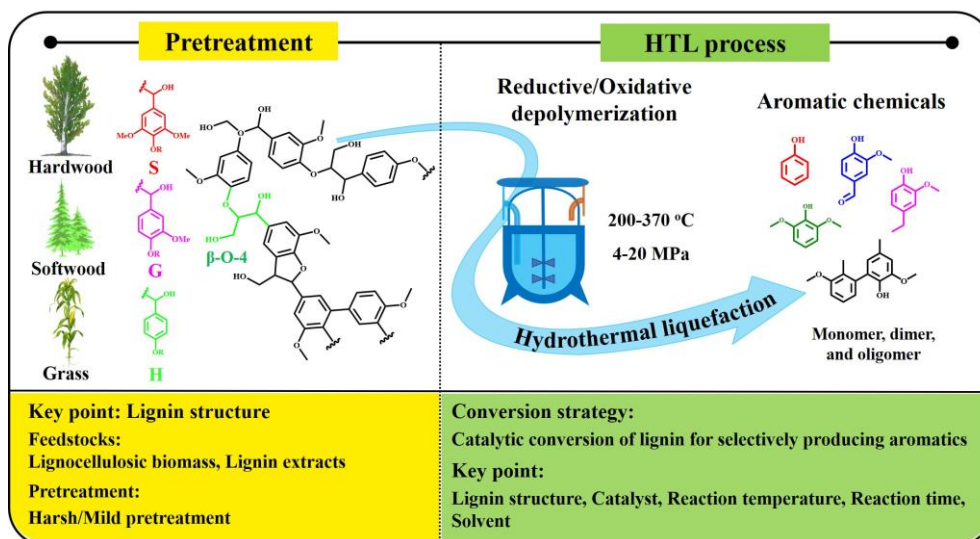
437 **Table 5.** Modification and application of hydrochar.

Modification approaches	Properties	Applications	Ref.
Chemical activation by KOH	High specific surface area	High-performance supercapacitor	[62]
Co-HTC of lignin with protein and chemical activation by KOH	Hierarchical pore structure; High specific surface area; Nitrogen doping	High-performance supercapacitor	[112]
Physical activation by CO ₂ and modification by NH ₃	High specific surface area; Nitrogen doping	Electrocatalytic oxygen reduction	[75]
Physical activation and use of soft template (P123 and F127)	High specific surface area; Porous structure	Ru-loaded carbon catalyst for xylose conversion	[114]
H ₂ SO ₄ -catalyzed HTC	Acidic groups	Meatal-free catalyst for fructose conversion	[87]
Impregnation of Al on hydrochar	Al-hydrochar with oxygenated functional group	Al-hydrochar catalyst for glucose isomerization	[115]
Co-HTC of leaves and Spirulina and activation by ZnCl ₂ /CO ₂	High specific surface area; Nitrogen doping; Ultra-micropores	CO ₂ adsorption	[111]

Chemical activation by KOH	High specific surface area	Gas storage	[77]
Co-HTC of food waste with yard waste	High energy density; High mass density	Solid biofuel	[116]
Microwave-assisted HTC	High energy density	Solid biofuel	[117]
Urea-assisted HTC and chemical activation by KOH	High specific surface area; Porous structure; Nitrogen doping	Pollutant adsorption	[39]
Acid-catalyzed HTC	Oxygen-rich functional groups	Organics adsorption	[110]
Zn(II)-catalyzed HTC	Oxygenated functional groups	Organics degradation	[72]

438 **4. Hydrothermal liquefaction**

439 For the HTL process of lignin-rich feedstock, selective production of aromatics depends on
440 the lignin source, specific reaction parameters, and catalysts used. The key factors involved in
441 lignin pretreatment are the biomass source and the pretreatment conditions that influence the
442 initial structure of lignin and govern its subsequent conversion. The lignin structure and
443 catalytic systems are the vital factors in the HTL process (**Fig. 6**). We first discuss the lignin
444 feedstock and its importance for the selective production, as well as the associated implications
445 for scale-up process. We then discuss the operating parameters and various catalysts developed
446 for the HTL process of lignin to specific aromatics.



447

448

Fig. 6. HTL of lignin-rich feedstock for production of aromatics.

449 4.1. Feedstock

450 4.1.1. Native lignin in lignocellulosic biomass

451 Lignocellulosic biomass and lignin extract involved in the HTL process are reviewed for the

452 aromatics production (**Table 6**). Reductive catalytic fractionation (RCF) has been explored for

453 the conversion of native lignin in lignocellulose, and the well-preserved carbohydrates are

454 suitable for further processing [118, 119]. High degree of delignification and high yields of

455 aromatic monomers could be achieved in RCF of lignocellulosic biomass [120]. However, this

456 strategy also resulted in the degradation or modification of carbohydrates, posing a

457 fundamental challenge in selective conversion process. The biomass variability adds to the

458 problems associated with structural complexity of lignin and its derived products. Various

459 analyses such as element analysis, FTIR, 2D NMR, and SEM have been used to characterize

460 the chemical, morphological, and structural properties of lignin sources. Specially, 2D HSQC

461 NMR is used to elucidate the initial structure of lignin in terms of S:G:H ratio and interunit

462 linkage distribution. Gel permeation chromatography can be used to analyze the molecular

463 weight distribution of lignin feedstock and its derived bio-oil. With the improved understanding
 464 of complex characteristics of lignin, it has been recognized in recent studies that its structure
 465 differs markedly owing to different biomass sources and pretreatment methods.

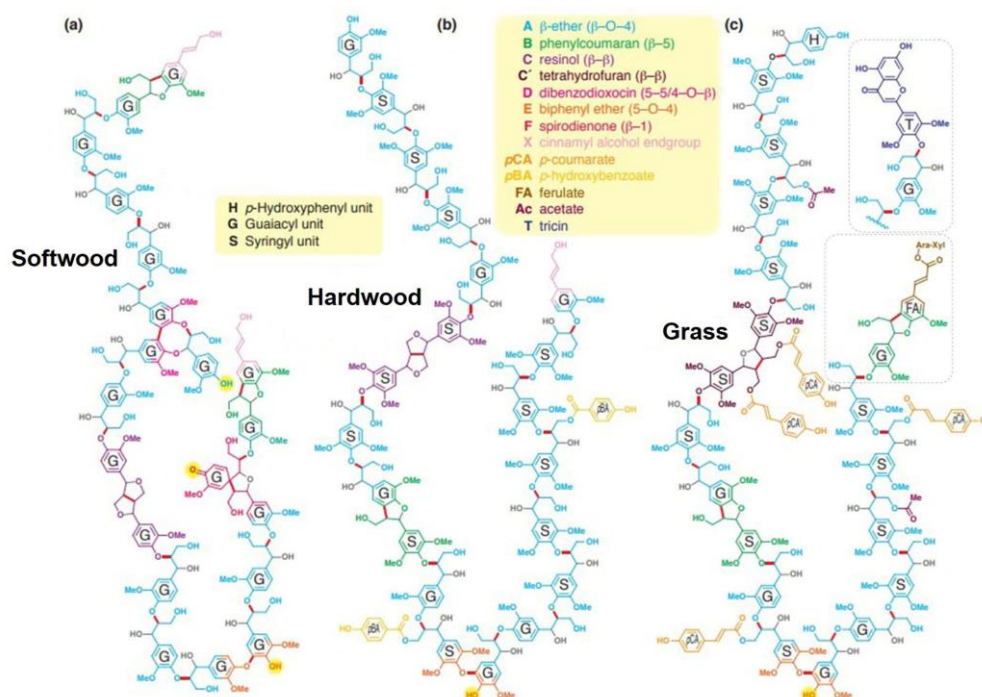
466 Lignin derived from softwood, hardwood, and grass possess different contents of S, G, and
 467 H units that are typically cross-linked through C-O and C-C bonds [43], as shown in **Fig. 7**.
 468 The S/G-rich lignin in hardwood is rich in β -O-4 linkage that is related to high-yield production
 469 of aromatic monomers [68]. Lignin in grass is mainly composed of S-G-H-type units, whereas
 470 lignin in softwood is mainly composed of G units that often lead to the formation of stable β - β
 471 and 5-5 linkages [121]. Because of the high content of G units, softwood lignin can be a
 472 potential feedstock for high selective production of G-type aromatics. Vanillin, as a building
 473 block for the chemical industry, has been produced from the oxidative conversion of softwood
 474 by using alkaline catalysts [122, 123]. With the recent development, monolignol *p*-coumarate
 475 (*p*CA) and ferulic acid (FA) moieties that are cross-linking agents between carbohydrates and
 476 lignin were detected in the fast-growing biomass, such as corn stalk and wheat straw [124-126].
 477 Due to its unique structure, several studies investigated the reactivity of *p*CA for the selective
 478 production of target aromatics [127, 128]. Lignin source is a crucial factor determining the
 479 native structures of lignin and the properties of resulting products. It is essential to scrutinize
 480 the structural variability of lignin feedstock and elucidate the key characteristics of lignin
 481 sources, β -O-4 linkage, and S:G:H ratio for designing an effective biorefinery strategy.

482 **Table 6.** Experimental investigation on the HTL of various lignin-rich feedstock.

Feedstock	Conditions	Catalyst	Key Findings	Ref.
Pine	160 °C, 1 h, 1 MPa O ₂	NaOH	Baes-catalyzed oxidation: Oxidative conversion of various lignocelluloses (<i>e.g.</i> , pine, eucalyptus, grass, and bagasse	[121]

Alkaline lignin	250 °C, 1 h, N ₂	Solid bases	waste) could produce both aromatics and cellulose. Pine gave a high yield of vanillin (21.1 wt%) and low-molecular oligo-phenolics (56.7%). Base-catalyzed reaction: Reaction temperature, time, and pressure could affect HTL of alkaline lignin over various solid bases. A high yield of low-molecular-weight products was obtained over basic NaX catalyst at 250 °C for 1 h.	[129]
Kraft lignin	200 °C, 30 min, 1.5 MPa O ₂	NaOH	Baes-catalyzed oxidation: The yields of organic acids and the contents of phenolic monomers, dimers, and trimers (<1 kDa) increased with the increase in oxygen pressure and temperature.	[130]
Organosolv lignin	300 °C, 80 min, 9 MPa	NaOH	Baes-catalyzed oxidation: HTL of different organosolv lignin from olive tree was investigated. Acetosolv lignin gave the highest yield of bio-oil (18.48 wt%), while formosolv lignin enabled a high yield of phenolic monomers (28.2%) in the bio-oil.	[131]
Bagasse lignin	260 °C, 15 min, N ₂	Acidic ionic liquid	Acid-catalyzed reaction: HTL of sugarcane bagasse lignin using [C ₄ H ₈ SO ₃ Hmim]HSO ₄ achieved 65% of delignification and yielded 13.5% of aromatic monomers, including phenol, guaiacol, and 4-ethylphenol.	[132]
Alkali lignin	160 °C, 7 min, 1 MPa O ₂	NaOH, CuSO ₄	Oxidation: The cleavage of C-O and C-C bonds in lignin was promoted in the presence of Cu ²⁺ to yield aromatic aldehydes and ketones. At high pH, depolymerization and condensation reactions occurred simultaneously and shared the reactive intermediates.	[133]
Dealkaline lignin	250 °C, 30 min, 0.7 MPa N ₂	Solid acids	Reduction: HTL process with various solid acid catalysts could convert different types of lignins into aromatic monomers under an inert atmosphere. Depolymerization of dealkaline lignin over the SiO ₂ -Al ₂ O ₃ catalyst achieved a high yield of phenolic monomers (60%).	[65]
Birch lignin	250 °C, 20 h,	Ru/Nb ₂ O ₅	Reduction: HTL of lignin over a Ru/Nb ₂ O ₅ catalyst produced a high yield	[134]

483



484

485 **Fig. 7.** Lignin structures in softwood, hardwood, and softwood [43].486 **4.1.2. Lignin extracts**

487 Selective lignin extraction from initial lignocelluloses could produce high-purity lignin

488 extracts. Wide-ranging pretreatments have been developed by using acids, bases, and organic

489 solvents. The harsh pretreatment can alter the H/G/S ratios and reduce the degree of

490 polymerization in order to remove lignin from biomass [53]. Studies on lignin extraction have

491 demonstrated that the lignin extracts containing variable aromatic rings and side chains are

492 more complex than their original structures [69, 135]. By far, the most common extraction

493 approaches are organosolv methods that employ an organic solvent for delignification.

494 Organosolv pretreatment can liberate lignin from biomass by cleaving ether and ester bonds

495 and forming C-OH groups with a mildly modified structure of lignin [136, 137]. Typical

496 thermal pretreatments such as hydrothermal liquefaction and steam explosion focus on the

497 production of monomeric carbohydrates and lead to the formation of more recalcitrant lignin
498 polymer. High-severity conditions using a strong acid/base similarly result in undesirable
499 condensation of lignin, and the recovered low-quality lignin is not suitable for subsequent
500 depolymerization. For example, Kraft lignin subjected to alkaline pretreatment in the pulp and
501 paper industry typically possesses a lower content of β -O-4 linkages but high contents of C-C
502 bonds and phenolic hydroxyl groups due to the cleavage of C-O bonds [69]. This process makes
503 the lignin recalcitrant for subsequent conversion. The microwave-assisted HTL of Kraft lignin
504 also gave low yields of aromatic monomers and bio-oils [53].

505 **4.2. Operating conditions**

506 **4.2.1. Operating parameters in reductive systems**

507 High oxygen content is one of the most significant barriers to biomass conversion into ideal
508 liquid biofuel. Hydrodeoxygenation (HDO) reaction can produce de-functional aromatics such
509 as arenes and phenolics from the lignin-rich feedstock. However, high-severity conditions
510 simultaneously facilitate the production of cycloalkanes through HDO reaction [80, 134, 138].
511 Shao et al. [134] explored the selective production of arenes *via* HDO of lignin over a
512 Ru/Nb₂O₅ catalyst at 250 °C for 10 h. Four phenolic monomers (total G-/S-type monomer
513 yields of 7.7 wt%) were obtained together with arenes and cycloalkane-based hydrocarbons
514 (total yields of 9.7 wt%). Hydrocarbon yields of 35.5 wt% with a selectivity of 71 wt% for
515 arenes was obtained after 20 h. This study suggested that birch lignin could be firstly
516 depolymerized to phenolic monomers *via* the cleavage of β -O-4 linkages, and the formed
517 phenolic monomers were sequentially converted to arenes and cycloalkanes by HDO over the
518 Ru/Nb₂O₅ catalyst. The promotional effect of high reaction temperatures on the cleavage of

519 C_{aromatic}-OH bonds over the Ru/Nb₂O₅ catalyst was also demonstrated by using lignin model
520 compounds.

521 Various reaction conditions were optimized by Liu et al. [120] through RCF of eucalyptus
522 to selectively produce phenolic compounds over the Ni@ZIF-8 catalyst. Lower reaction
523 temperature (or performing the reaction under the N₂ atmosphere) sharply reduced monomer
524 yields along with a significant drop in the delignification degree. Chaudhary et al. [129]
525 investigated the effects of reaction time, temperature, and pressure on the base-catalyzed
526 depolymerization of lignin into low-molecular-weight aromatics. Maximum yield (51%) of
527 low-molecular-weight products was achieved at 250 °C after 1 h, but the yields started
528 declining with a decrease in temperature or a longer reaction time. At high temperatures, the
529 decline in monomer yields might be not only associated with the temperature effect but also
530 affected by the pressure changes. Increasing the reaction pressure by 0.3 MPa of N₂ at a fixed
531 temperature promoted the lignin depolymerization towards high-yield aromatics production.
532 Zhang et al. [80] found that the hydrogenation of benzene to cyclohexane occurred when the
533 H₂ pressure was over 1 MPa, implying the direct deoxygenation and deep HDO reactions
534 become more dominant at higher severity.

535 **4.2.2. Operating parameters in oxidative systems**

536 For oxidative systems, the major challenge for the selective production of aromatics is to
537 overcome stronger oxidation or condensation of reactive products [130, 139, 140]. High
538 temperatures or O₂ pressures could increase the yields of phenol-derived chemicals, and
539 organic acids such as formic and acetic acids resulted probably from HTL of Kraft lignin [130].
540 At a high temperature, lignin depolymerization becomes more complex as the secondary

541 reactions occur, and the condensation of reactive intermediates leads to the formation of stable
542 C-C bonds. The study of microwave-assisted wood degradation highlighted the strong
543 influence of reaction temperature on vanillin production [123]. High temperatures significantly
544 promoted lignin conversion and enabled high yields of vanillin and vanillic acid. The yields of
545 vanillic acids decreased when the reaction temperature was higher than 200 °C, implying that
546 the oxidation of vanillin was hindered and the condensation became more dominant at high
547 severity. Vanillin yields were hardly affected by a longer reaction time.

548 Previous studies also investigated the influence of O₂ pressure on the product yields. A higher
549 O₂ pressure enabled lignin depolymerization into aromatic monomers at a lower temperature
550 (120 °C) [139]. Nonaromatic carboxylic acids were formed as the secondary breakdown
551 products from subsequent oxidation of lignin-derived aromatics under severe conditions. High
552 reaction pressures could suppress the formation of oligomers more significantly than
553 monomers [140, 141]. The negative effect of pressure on the monomer yields was ascribed to
554 the solvent-cage effect from the high density of water under high pressures, resulting in
555 stronger intermolecular interactions and limited diffusion of soluble reactants [21, 22].
556 Therefore, the reaction pathways in subcritical water would change with the increase of water
557 density under high pressures. Hafezisefat et al. [140] investigated the oxidative cracking with
558 O₂ to convert lignin into phenolic monomers by using various solvents to increase the oxygen
559 solubility. They reported that increasing O₂ pressure from 50 psi (0.34 MPa) to 300 psi (2.07
560 MPa) could improve the yields of vanillin and syringaldehyde from 6.0 wt% to 10.5 wt%.
561 Meanwhile, deep oxidation of aromatic aldehydes was promoted with the formation of
562 corresponding aromatic acids. In addition, enhanced water density at high pressures might

563 result in higher dissolution capacity to dissolve more organic compounds but with limited
564 diffusion ability [23].

565 **4.3. Catalysts**

566 **4.3.1. Homogeneous catalysts**

567 The HTL process of lignin has been widely studied using various homogeneous bases (*e.g.*,
568 NaOH, KOH, and Na₂CO₃), metal salts (*e.g.*, CuSO₄, CuCl₂, and MnCl₂), water-soluble metal
569 complexes, and ionic liquids (ILs) [131, 133, 141-143]. Experimental investigations on the
570 base-catalyzed depolymerization of various lignin-rich feedstock *via* HTL process are listed in
571 **Table 6**. Erdocia et al. [131] performed HTL of lignin in a 4 wt% of NaOH solution and
572 investigated the influence of different organosolv lignin on the oil production. Lignin extracted
573 from acetosolv pulping gave the highest bio-oil yields of 18.5%. In addition to the cleavage of
574 β -O-4 linkage, the dealkylation of side chains occurred along with the formation of phenol,
575 cresols and catechol. Oxidative depolymerization of Kraft lignin was investigated by Abdelaziz
576 et al. [130], in which low-molecular-weight chemicals, mainly consisting of aromatic
577 monomers and carboxylic acids, were produced at high O₂ pressures. Zhu et al. [121] reported
578 efficient delignification of softwood, hardwood, and grass for the selective production of
579 vanillin and cellulose by oxidative biorefining in a 7.5 wt% of NaOH solution. Under the
580 optimal condition, 90% of lignin could be converted into aromatics. Various operating
581 conditions were explored by Roberts et al. [141] to elucidate the detailed mechanisms of base-
582 catalyzed depolymerization. The presence of Na⁺ could react with lignin and form cation
583 adducts and then polarize β -O-4 linkages, leading to the heterolytic cleavage of C-O bonds and
584 the release of monomers.

585 In addition to homogeneous bases for lignin liquefaction, the acid-catalyzed strategy has
586 attracted extensive attention due to simultaneous delignification and conversion of
587 lignocellulosic biomass in this process [144-146]. Dilute aqueous acids such as H₂SO₄, H₃PO₄,
588 and organic acids could promote hydrolysis and delignification of lignocelluloses, resulting in
589 the formation of soluble lignin fragments that were subsequently converted into aromatics
590 [147]. The latest studies reported that small organic acids, such as formic acid and acetic acid,
591 could act as *in situ* hydrogen donors, thus reducing the demand for external hydrogen to
592 upgrade lignin [148, 149]. A novel acidic IL as a homogeneous catalyst was explored by Long
593 et al. [132, 150] for lignocellulosic biomass conversion. The results demonstrated that acidic
594 IL possessed excellent cleavage capability of C-O bonds and particularly promoted the
595 degradation of G- and S-lignin due to the formation of cooperative IL pair with G-/S-type units
596 in the lignin structure.

597 **4.3.2. Heterogeneous catalysts**

598 Heterogeneous catalysts such as metals, metal oxides, and carbon-based materials have been
599 explored in the HTL process for their easy separation and recovery [53, 120, 138]. A wide range
600 of support (*e.g.*, Nb₂O₅, ZrO₂, Al₂O₃, TiO₂, HZSM-5, and activated carbon) were used to
601 prepare Ru-based catalysts and tested for HTL of organosolv birch lignin [134]. The yield of
602 C₇-C₉ hydrocarbons over the Ru/Nb₂O₅ catalyst was 35.5 wt% with a high selectivity of 71 wt%
603 for arenes. The other catalysts showed a decrease in both yields of C₇-C₉ hydrocarbons and
604 selectivity of arenes. Over the Ru/Al₂O₃ catalysts, the yields of C₇-C₉ products decreased to
605 18.3 wt%. The C₇-C₉ arenes were not detected when using the Ru/C catalyst. This work
606 highlighted the synergy between the Ru and Nb₂O₅ species that enabled simultaneous

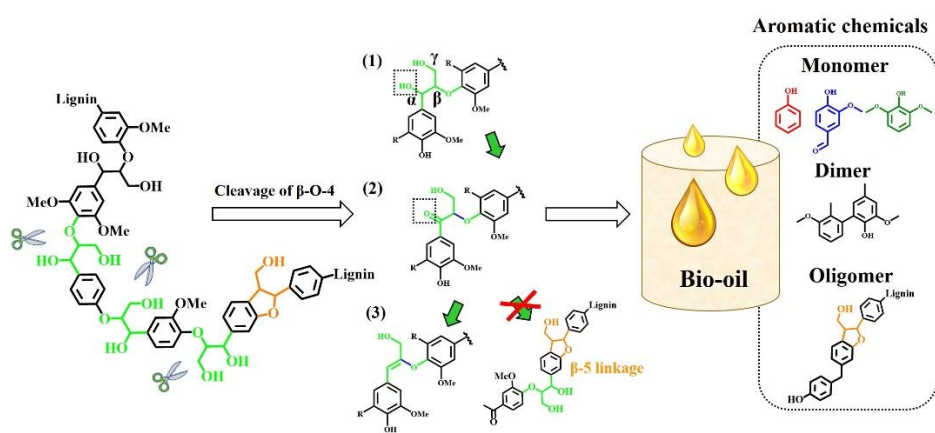
607 depolymerization and hydrogenolysis of organosolv lignin *via* the selective cleavage of β -O-4
608 linkages in lignin and C_{aromatic}-OH bonds in phenolic monomers. Accordingly, Zhang et al. [80]
609 prepared Ru/Nb₂O₅-MC (micro-mesoporous carbon) catalyst with the enhanced pore structure
610 to further improve its catalytic activity. The hydrophobic MC and hydrophilic Nb₂O₅
611 contributed to the formation and stabilization of Pickering emulsions in the biphasic process,
612 where the selective cleavage of C_{aromatic}-OH bonds could occur.

613 A variety of heterogeneous catalysts based on non-precious metals (*e.g.*, Co, Ni, Cu, and Fe)
614 have been widely explored [27, 150, 151]. Different mesoporous zeolites supported metal
615 catalyst (Ni/MCM, Al/MCM-41, and Ni-Al/MCM-41) were explored in the HTL of Kraft
616 lignin [27]. The maximum bio-oil yield of 44.3 wt% was obtained in the presence of Ni-
617 Al/MCM-41 catalyst. The high carbon contents of bio-oils were obtained as 84.2%, 81.4%, and
618 80.3% using water, ethanol, and methanol as solvents, respectively, indicating the promotion
619 of oil deoxygenation over Ni-based catalysts. For the oxidative reaction, Cu-based catalyst
620 exhibited excellent activity in the dehydrogenation of biomass feedstock [152-154]. The
621 coexistence of Cu⁺ and Cu⁰ provided a high activity and played different roles in O₂-rich and
622 H₂-rich streams. Feng et al. [155] demonstrated the Cu⁺-Cu⁰ bicomponent CuNPs@ZIF-8
623 catalyst contributed to the high activity for selective hydrogenation of HMF. The aldehyde
624 could be adsorbed by the electron-deficient Cu⁺ species while H₂ could be dissociated at Cu⁰
625 via hydrogen spillover effect to achieve efficient hydrogenation. The promotional effect of the
626 coexistence of Cu⁺ and Cu⁰ in the CuO/BCN catalyst was reported in the oxidative conversion
627 of lignin [53]. The strong metal-support interaction contributed to the cleavage of C-O bonds
628 through dehydrogenation reaction. Various solid acid catalysts (*e.g.*, H-USY, H-ZSM-5, H-

629 BEA, and K10 clay) could assist the cleavage of ether bonds and the removal of functional
 630 groups such as hydroxyl, carboxyl, and methoxy groups [65]. Typical basic zeolites, such as
 631 NaX, NaP, and KLTL, were explored for improving the lignin depolymerization and the NaX
 632 catalyst under the lower reaction temperature gave the best oil yield (51%) at 250 °C for 1 h
 633 [129].

634 4.4. Fundamental mechanisms

635 Based on the latest studies [156-159], the reaction pathways for HTL of native lignin within
 636 β -O-4 structures are illustrated in **Fig. 8**. The conversion of native lignin aimed to cleave C-O
 637 bonds in β -O-4 motifs. (1) In general, C_{α} -OH undergoes hydrogenolysis in β -O-4 linkages. (2)
 638 The oxidation C_{α} -OH to C_{α} =O through dehydrogenation reaction can lower the dissociation
 639 energy of C_{β} -O bond from 247.9 to 161.1 kJ mol⁻¹ but lead to notably higher dissociation energy
 640 of C_{α} - C_{β} (294.2 kJ mol⁻¹), making it harder to be cleaved [159]. (3) The newly formed C_{α} ketone
 641 undergoes dehydration reaction to generate an enol ether intermediate, and the weakened C_{β} -
 642 O bond can be cleaved by hydrolysis or hydrogenolysis, thus releasing small and degraded
 643 fragments.



644

645 **Fig. 8.** Pathways for the cleavage of β -O-4 linkages into aromatics.

646 Native lignin and its extract typically undergo a series of chemical reactions, including
647 hydrolysis, cleavage, and condensation during its biosynthesis and chemical fractionation,
648 resulting in various contents of C-O and C-C bonds in their structures. For example, Kraft
649 lignin structures recovered from the pulp industry was tremendously modified, which
650 significantly limited the monomer yield due to the formation of robust C-C bonds by alkaline
651 pretreatment [160]. For native lignin, several studies investigated the protection strategies by
652 using formic acid or formaldehyde to stabilize the highly reactive intermediates and inhibit the
653 formation of C-C bonds [157, 158]. However, lignin extracts have existed a large amount of C-
654 C bonds in the structures. The selective cleavage of C-C bonds using effective catalysts was
655 studied to provide new insights into lignin valorization with broad applicability. Stein et al.
656 [161] reported that Ru-based complexes exhibited a high selectivity in the cleavage of C-C
657 bonds in 1,3-dilignol model compounds. Dong et al. [162] explored the catalytic cleavage of
658 both interunit C-C and C-O bonds over the Ru/NbOPO₄ catalyst. The abundant Brønsted acid
659 sites in the phosphate-based catalyst can protonate the benzene rings in the 5-5 C-C bonds in
660 biphenyl, as a lignin model compound, and thus facilitate the cleavage of C-C bonds.

661 **5. Techno-economic assessment**

662 Recent studies have conducted techno-economic assessment (TEA) for the production of
663 biofuel and bio-products from lignocellulosic biomass [163, 164]. For the HTC process of yard
664 waste, process models were developed for two different HTC plant configurations that included
665 flash separators (case A) and heat exchangers (case B). In terms of costs, the price for case A
666 was \$3.3 per GJ more than that in case B, but case A was preferable in terms of energy
667 production [165]. For case B, increasing plant capacity from 9.6 to 960 tons per day

668 significantly decreased the cost of production from \$47.2 to \$4 per GJ. The TEA results of
669 HTC of food waste mixed with coal revealed that the break-even costs would be \$60.26, \$62.24,
670 and \$69.90 per ton for handling food waste, coal, and mixture of food waste and coal,
671 respectively. The costs associated with raw feedstock collection and transportation were crucial
672 factors that significantly affected the corresponding break-even costs [166]. Mahmood et al.
673 [167] identified the key factors affecting profitability of hydrochar production from food waste
674 (2000 tons per day) based on the TEA results. The sensitivity analysis revealed that both bio-
675 oil yield and cost of enzyme for pretreatment had a significant impact on the selling price of
676 hydrochar, and the minimum selling price of products from non-enzyme pretreated (\$30 per
677 ton) is less than half of the market price (\$85.68 per ton). The results from TEA of HTC of
678 green waste showed that the hydrochar product could economically compete with fossil-
679 derived biofuel in an optimal context [168]. Besides, the potential for reducing GHG emissions
680 was evident compared with the processing of fossil sources [4]. Nevertheless, there is still a
681 large potential for cost saving by reducing the costs related to the transformation and full
682 utilization of selected biomass feedstock and its residue and byproducts.

683 For the HTL process of lignocellulosic biomass, Liao et al. [16] designed a process model
684 to perform a TEA study for converting 1000 kg of birch wood into 653 kg of carbohydrate pulp,
685 64 kg of lignin oligomers, 42 kg of phenol, and 20 kg of propylene. The cost of feedstock (birch
686 wood, €158 per ton) showed the highest contribution to the manufacturing costs, whereas the
687 cost of recyclable catalysts could be negligible. Furthermore, shorter reaction time and higher
688 substrate loading ratio were considered to be essential factors for improving the profitability of
689 the process, which required the design of a more efficient HTL reactor. Vanillin production

690 from Kraft lignin was the only established HTL process to valorize the lignin waste from paper
691 pulp and produce valuable chemicals [169]. In terms of the economic aspect, the optimal
692 process conditions were the concentration of 30 g/L of lignin feedstock with low operating
693 temperature at 130 °C and oxygen partial pressure of 0.5 MPa, then the payback period for the
694 investment would be 6.2 years. Additional TEA of the HTL of oil from lignin for the BTEX
695 (benzene, toluene, ethylbenzene, and xylenes) production of 65-70 million liters per year was
696 explored [170]. The results showed that the minimum selling price of BTEX was between \$1.65
697 and \$2.00 per liter. Further research efforts are required for reducing the oxygen content of bio-
698 oil through HDO reaction and decreasing the HTL operating costs in order to render biofuel
699 products more economically competitive with fossil-based fuels in the market.

700 **6. Challenges and perspectives**

701 The hydrothermal processing of lignocellulosic biomass into fuels and value-added products
702 has received renewed emphasis thanks to recent advances and better understanding of the
703 complex characteristics of feedstock variability, reaction mechanisms and pathways, and
704 properties of target products and byproducts. Although considerable efforts have been made in
705 fundamental research and technology development at a laboratory scale, inherent challenges
706 associated with biomass heterogeneity still impede its large-scale implementation. HTC
707 process has been industrialized for selected biomass, but HTL process is yet to be
708 commercialized due to the technological challenges (*e.g.*, high pressure and harsh chemical
709 environment). The major challenges and future perspectives are discussed as follows:

710 **6.1. Challenges**

711 (1) Various types of biomass contain a wide diversity in compositions and chemical

712 structures of cellulose, hemicellulose, and lignin, as described in Section 2. The interactions
713 among these components and process severities differ in the hydrothermal process, resulting in
714 less-efficient conversion and simultaneous production of mixed products. Subsequent efforts
715 required for separation and purification of mixed products would be crucial for achieving cost-
716 effective and sustainable biorefinery towards industrial-scale implementation.

717 (2) Selection of lignocellulose biomass is a crucial factor associated with both chemical and
718 physical challenges in HTL and HTC processes. The impact of chemical aspects, including
719 compositions, structures, and properties of biomass feedstock, and technological parameters
720 such as reaction temperature, ramping and holding time, and heat and mass transfer rate, etc.,
721 have to be extensively studied for a holistic understanding. Some less-investigated physical
722 parameters of biomass feedstock (particle size, mass density, mechanical strength. etc.) and
723 economic issues (reactor design, liquid-to-solid ratio, mixing regime, catalyst stability/recovery,
724 product separation/purification, etc.) play crucial roles in the scale-up of the hydrothermal
725 process. They are currently less explored and the information gaps between the laboratory and
726 industry scales should be addressed.

727 (3) Lignin-derived bio-oil typically contains abundant aromatic monomers associated with
728 the cleavage of β -O-4 linkages. Besides lignin monomers, the remaining fractions include
729 dimers and oligomers derived from C-C bond-linked units or repolymerization of reactive
730 monomeric intermediates. Using GC-MS and LC-MS can only identify and quantify monomers
731 and dimers, whereas the analysis of oligomers in the liquid phase still poses a technical
732 challenge.

733 (4) Hydrochar is a temperature-sensitive material, and its characteristics can be greatly

734 altered when subjected to high reaction temperatures. Increasing the hydrothermal temperature
735 will form a parallel network of varying reaction pathways of degradation of different
736 components in lignocellulosic biomass. As a result, monosaccharides, polysaccharides, organic
737 acids, and humins are simultaneously formed. The fate and value-added utilization of the
738 polysaccharides and humins have been little explored [170]. Improved analytics are required
739 for obtaining new insights into the reaction mechanisms and pathways for hydrochar
740 customization and broader application.

741 (5) The transformation of minor species (*e.g.*, N, P, Si, K, Na, Mg, and Ca) is often ignored
742 in the HTC process. These inorganic species can affect (or catalyze) the formation pathways of
743 hydrochar and the distribution of products/by-products. A significant quantity of wastewater
744 (process water) that is rich in organic compounds should be recycled as much as possible and
745 carefully treated before final discharge. For example, a few recent studies have used the process
746 water for anaerobic digestion to produce biogas afterwards.

747 **6.2 Future perspectives**

748 To overcome the technological challenges, future studies should elucidate the crosslinking
749 influences of biomass variability on the production of biofuels/bioproducts and develop
750 product-oriented solutions to address the heterogeneity of lignocellulosic biomass. Advanced
751 characterization of the molecular structures and properties of oligomers can improve the
752 holistic design of downstream valorization strategies. It is imperative to standardize the
753 feedstock provision (*e.g.*, characterization protocols and material specifications) and develop
754 reaction models and process flow designs that consider the biomass compositions and
755 determine the hydrothermal temperature, time, loading, mixing, solvent, pressure, and catalyst

756 required to accomplish the selective conversion. Rational selection of various types of
757 lignocellulosic biomass should be based on our deep understanding of the properties of raw
758 feedstock and targeted biofuels/bioproducts.

759 Homogeneous and heterogeneous catalysis is of paramount significance for high-efficiency
760 energy production and chemical transformation. Their applicability and limitations in the
761 hydrothermal process are discussed in Sections 3&4 and summarized in **Table 7**.
762 Homogeneous catalysis has been extensively investigated. The main drawback is that mineral
763 acids can cause equipment corrosion, catalyst wastage, wastewater treatment, and
764 environmental impacts. Heterogeneous reactions depend on the properties of biomass
765 feedstock, operating temperature, and atmosphere of the reaction system, etc. Understanding
766 and tailoring the chemical states of the solid catalysts and conversion pathways of substrates
767 with the assistance of *in situ* characterization and advanced material synthesis can put us in a
768 better position to design more energy-efficient catalytic systems. New development in catalyst
769 design (*e.g.*, highly selective and recyclable catalysts) and heterogeneous systems can foster
770 the innovation and broad application of sustainable engineering solutions. Overall, cost-
771 effective and eco-friendly engineering designs of catalytic hydrothermal process require our
772 concerted efforts in the future studies on fundamental research extending the frontiers of
773 knowledge.

774 **Table 7.** Applicability and limitations of homogeneous and heterogeneous catalysis for
775 sustainable conversion of lignocellulosic biomass.

Reaction	Key Factors	Applicability	Limitations
Homogeneous catalysis	Active species, Solvent system,	High activity, Solvent effect,	Equipment corrosion, Difficult separation,

	Temperature,	Uniform dispersion,	Poor reusability,
	Reactor design	Various biomass feedstock	Low selectivity
Heterogeneous	Biomass feedstock,	Easy separation,	Low hydrothermal stability,
catalysis	Particle size,	Well-defined structure,	Limited contact with
	Temperature,	Multiple active sites,	feedstock,
	Atmosphere	High selectivity	Low active atom utilization

776 The keys to the implementation of hydrothermal technologies on a larger scale are related to
777 economics, performance, and environmental footprints. Economics is critical for biofuel as it
778 has already been proven to exhibit similar performance and greater environmental friendliness
779 compared with petroleum-derived counterparts. Continued development of fundamental and
780 translational research as well as further establishment of worldwide bio-based economy will
781 be vital for the scale-up hydrothermal processes. All of the above rely on our effective and
782 interdisciplinary collaboration in the future.

783 **7. Conclusions**

784 Hydrothermal treatment of biomass has been extensively studied as a biorefinery technology
785 for producing solid hydrochar and liquid bio-oil with high chemical functionality. In this
786 critical review, we articulate the key factors (*e.g.*, feedstock variability, reaction temperature,
787 time, and catalyst) that determine the nature and properties of solid and liquid biofuel in the
788 HTC and HTL processes. In particular, we critically review the influences of feedstock
789 compositions and chemical structures on the selective production of value-added chemicals
790 and multifunctional hydrochar. Temperature is a crucial parameter to determine the degree of
791 carbonization and liquefaction. Catalysis plays a key role in governing the physicochemical
792 properties of hydrochar, improving the product yields, and facilitating the selective production

793 of aromatics. The hydrochar with desirable functionalization can enable broad applications in
794 catalysis, energy storage, and environmental fields. A wide range of aromatics from HTL of
795 lignin-rich feedstock with homogeneous or heterogeneous catalysts can closely resemble
796 petroleum-derived fuels. The state-of-the-art developments, current challenges, and future
797 perspectives of hydrothermal processes presented in this review will advance our fundamental
798 knowledge of sustainable chemistry for maximizing the carbon-efficient valorization of
799 biomass resources towards bio-based circular economy.

800

801 **Acknowledgement**

802 The authors appreciate the financial support from the Hong Kong Environment and
803 Conservation Fund (ECF Project 101/2020) and Hong Kong Research Grants Council (PolyU
804 15222020).

805

806 **References**

- 807 [1] Zimmerman JB, Anastas PT, Erythropel HC, Leitner W. Designing for a green
808 chemistry future. *Science* 2020;367:397-400.
- 809 [2] Mirmohamadsadeghi S, Karimi K, Azarbaijani R, Parsa Yeganeh L, Angelidaki I,
810 Nizami A-S, Bhat R, Dashora K, Vijay VK, Aghbashlo M, Gupta VK, Tabatabaei M.
811 Pretreatment of lignocelluloses for enhanced biogas production: A review on
812 influencing mechanisms and the importance of microbial diversity. *Renew Sustain*
813 *Energy Rev* 2021;135:110173.
- 814 [3] Petridis L, Smith JC. Molecular-level driving forces in lignocellulosic biomass
815 deconstruction for bioenergy. *Nature Rev Chem* 2018;2:382-389.
- 816 [4] Yang Y, Tilman, D. Soil and root carbon storage is key to climate benefits of bioenergy
817 crops. *Biofuel Res J* 2020;7:1143-1148.

- 818 [5] Yu, IKM, Chen H, Abeln F, Auta H, Fan J, Budarin VL, Clark JH, Parsons S, Chuck CJ,
819 Zhang S. Chemicals from lignocellulosic biomass: A critical comparison between
820 biochemical, microwave and thermochemical conversion methods. *Crit Rev Environ*
821 *Sci Technol* 2020;51:1479.
- 822 [6] Usmani Z, Sharma M, Karpichev Y, Pandey A, Chander Kuhad R, Bhat R, Punia R,
823 Aghbashlo M, Tabatabaei M, Gupta VK. Advancement in valorization technologies to
824 improve utilization of bio-based waste in bioeconomy context. *Renew Sustain Energy*
825 *Rev* 2020;131:109965.
- 826 [7] Liu W, You, W Sun W, Yang W, Korde A, Gong Y, Deng Y, Ambient-pressure and low-
827 temperature upgrading of lignin bio-oil to hydrocarbons using a hydrogen buffer
828 catalytic system. *Nature Energy* 2020;5:759-767.
- 829 [8] Zhang XG, Wilson K, Lee AF, Heterogeneously Catalyzed Hydrothermal Processing of
830 C₅-C₆ Sugars. *Chem Rev* 2016;116:12328-12368.
- 831 [9] Chen SS, Maneerung T, Tsang DCW, Ok YS, Wang C-H, Valorization of biomass to
832 hydroxymethylfurfural, levulinic acid, and fatty acid methyl ester by heterogeneous
833 catalysts. *Chem Eng J* 2017;328:246-273.
- 834 [10] Yu IKM, Tsang DCW, Yip ACK, Hunt AJ, Sherwood J, Shang J, Song H, Ok YS, Poon
835 CS. Propylene carbonate and γ -valerolactone as green solvents enhance Sn(IV)-
836 catalysed hydroxymethylfurfural (HMF) production from bread waste. *Green Chem*
837 2018;20:2064.
- 838 [11] Chen SS, Cao Y, Tsang DCW, Tessonnier J-P, Shang J, Hou D, Shen Z, Zhang S, Ok
839 YS, Wu KCW. Effective Dispersion of MgO Nanostructure on Biochar Support as a
840 Basic Catalyst for Glucose Isomerization. *ACS Sustainable Chem Eng* 2020, 8, (18),
841 6990-7001.
- 842 [12] Yu IKM, Xiong X, Tsang DCW, Wang L, Hunt AJ, Song H, Shang J, Ok YS, Poon CS.
843 Aluminium-biochar composites as sustainable heterogeneous catalysts for glucose
844 isomerization in a biorefinery. *Green Chem* 2019;21:1267-1281.
- 845 [13] Hu J, Zhang Q, Lee DJ. Kraft lignin biorefinery: A perspective. *Bioresour Technol*
846 2018;247:1181-1183.

- 847 [14] Abu-Omar MM, Barta K, Beckham GT, Luterbacher JS, Ralph J, Rinaldi R, Román-
848 Leshkov Y, Samec JSM, Sels BF, Wang F, Guidelines for performing lignin-first
849 biorefining. *Energy Environ Sci* 2021;14:262-292.
- 850 [15] Wu X, Fan X, Xie S, Lin J, Cheng J, Zhang Q, Chen L, Wang Y. Solar energy-driven
851 lignin-first approach to full utilization of lignocellulosic biomass under mild conditions.
852 *Nature Catal* 2018;1:772-780.
- 853 [16] Liao YH; Koelewijn SF, Bossche GVD, Aelst JV, Bosch SVD, Renders T, Navare T,
854 Nicolai T, Aelst VK, Maarten M, Matsushima H, Thevelein JM, Acker KV, Lagrain B,
855 Verboekend D, Sels BF. A sustainable wood biorefinery for low-carbon footprint
856 chemicals production. *Science* 2020;367:1385-1390.
- 857 [17] Liu B, Rajagopal D, Life-cycle energy and climate benefits of energy recovery from
858 wastes and biomass residues in the United States. *Nature Energy* 2019;4:700-708.
- 859 [18] Linger JG, Vardon DR, Guarnieri MT, Karp EM, Hunsinger GB, Franden MA, Johnson
860 CW, Chupka G, Strathmann TJ, Pienkos PT, Beckham GT. Lignin valorization through
861 integrated biological funneling and chemical catalysis. *Proc Natl Acad Sci*
862 2014;111:12013.
- 863 [19] Martinez CLM, Sermyagina E, Saari J, Jesus MSD, Vakkilainen EK. Hydrothermal
864 carbonization of lignocellulosic agro-forest based biomass residues. *Biomass*
865 *Bioenergy* 2021;147:106004.
- 866 [20] Sharma HB, Sarmah AK, Dubey B. Hydrothermal carbonization of renewable waste
867 biomass for solid biofuel production: A discussion on process mechanism, the influence
868 of process parameters, environmental performance and fuel properties of hydrochar.
869 *Renew Sustain Energy Rev* 2020;123:109761.
- 870 [21] Yang C, Wang S, Yang J, Xu D, Li Y, Li J, Zhang Y, Hydrothermal liquefaction and
871 gasification of biomass and model compounds: a review. *Green Chem* 2020;22:8210-
872 8232.
- 873 [22] Zhao Z, Bababrik R, Xue W, Li Y, Briggs NM, Nguyen D-T, Nguyen U, Crossley SP,
874 Wang S, Wang B, Resasco DE. Solvent-mediated charge separation drives alternative
875 hydrogenation path of furanics in liquid water. *Nat Catal* 2019;2:431-436.

- 876 [23] Gu X, Martinez-Fernandez JS, Pang N, Fu X, Chen S, Recent development of
877 hydrothermal liquefaction for algal biorefinery. *Renew Sustain Energy Rev*
878 2020;121:109707.
- 879 [24] Tekin K, Karagöz S, Bektaş S. A review of hydrothermal biomass processing. *Renew*
880 *Sustain Energy Rev* 2014;40:673-687.
- 881 [25] Zhang Y, Jiang Q, Xie W, Wang Y, Kang J, Effects of temperature, time and acidity of
882 hydrothermal carbonization on the hydrochar properties and nitrogen recovery from
883 corn stover. *Biomass and Bioenergy* 2019;122:175-182.
- 884 [26] Śliz M, Wilk M. A comprehensive investigation of hydrothermal carbonization Energy
885 potential of hydrochar derived from Virginia mallow. *Renew Energ* 2020;156:942-950.
- 886 [27] Feng L, Li X, Wang Z, Liu B. Catalytic hydrothermal liquefaction of lignin for
887 production of aromatic hydrocarbon over metal supported mesoporous catalyst.
888 *Bioresour Technol* 2021;323:124569.
- 889 [28] Watson J, Wang T, Si B, Chen W-T, Aierzhati A, Zhang Y, Valorization of hydrothermal
890 liquefaction aqueous phase: pathways towards commercial viability. *Prog Energy*
891 *Combust Sci* 2020;77:100819.
- 892 [29] Sikarwar VS, Zhao M, Clough P, Yao J, Zhong X, Memon MZ, Shah N, Anthony EJ,
893 Fennell PS, An overview of advances in biomass gasification. *Energy Environ Sci*
894 2016;9: 2939-2977.
- 895 [30] Roy P, Dutta A, Gallant J. Evaluation of the life cycle of hydrothermally carbonized
896 biomass for energy and horticulture application. *Renew Sustain Energy Rev Reviews*
897 2020;132:110046.
- 898 [31] Nicolae SA, Au H, Modugno P, Luo H, Szego AE, Qiao M, Li L, Yin W, Heeres HJ,
899 Berge N, Titirici MM. Recent advances in hydrothermal carbonisation: from tailored
900 carbon materials and biochemicals to applications and bioenergy. *Green Chem*
901 2020;22:4747-4800.
- 902 [32] Galadima A, Muraza O. Hydrothermal liquefaction of algae and bio-oil upgrading into
903 liquid fuels: Role of heterogeneous catalysts, *Renew Sustain Energy Rev* 2018;81:
904 1037-1048.

- 905 [33] Meng Q, Yan J, Wu R, Liu H, Sun Y, Wu N, Xiang J, Zheng L, Zhang J, Han B,
906 Sustainable production of benzene from lignin. *Nat Commun* 2021;12:4534.
- 907 [34] Yan J, Oyedeji O, Leal JH, Donohoe BS, Semelsberger TA, Li C, Hoover AN, Webb E,
908 Bose EA, Zeng Y, Williams L, Schaller KD, Sun N. Ray AE, Tanjore D. Characterizing
909 Variability in Lignocellulosic Biomass: A Review. *ACS Sustainable Chem Eng*
910 2020;8:8059.
- 911 [35] Kunkes EL, Simonetti DA, West RM, Serrano-Ruiz JC, Gartner CA, Dumesic JA.
912 Catalytic Conversion of Biomass to Monofunctional Hydrocarbons and Targeted
913 Liquid-Fuel Classes. *Science* 2008;322:417.
- 914 [36] Zhao X, Zhou H, Sikarwar VS, Zhao M, Park AHA, Fennell PS, Shen L, Fan LS.
915 Biomass-based chemical looping technologies: the good, the bad and the future. *Energy*
916 *Environ Sci* 2017;10:1885-1910.
- 917 [37] Ren S, Usman M, Tsang DCW, O-Thong S, Angelidaki I, Zhu X, Zhang S, Luo G.
918 Hydrochar-Facilitated Anaerobic Digestion: Evidence for Direct Interspecies Electron
919 Transfer Mediated through Surface Oxygen-Containing Functional Groups. *Environ*
920 *Sci Technol* 2020;54:5755-5766.
- 921 [38] Zhu X, Liu Y, Luo G, Qian F, Zhang S, Chen J. Facile fabrication of magnetic carbon
922 composites from hydrochar via simultaneous activation and magnetization for triclosan
923 adsorption. *Environ Sci Technol* 2014;48:5840-8.
- 924 [39] Xiao K, Liu H, Li Y, Yang G, Yao H. Excellent performance of porous carbon from
925 urea-assisted hydrochar of orange peel for toluene and iodine adsorption. *Chem Eng J*
926 2020;382:122997.
- 927 [40] Matsagar BM, Wang ZY, Sakdaronnarong C, Chen SS, Tsang DCW, Wu KCW. Effect
928 of Solvent, Role of Formic Acid and Rh/C Catalyst for the Efficient Liquefaction of
929 Lignin. *ChemCatChem* 2019;11:4604-4616.
- 930 [41] Changi SM, Faeth JL, Mo N, Savage PE. Hydrothermal Reactions of Biomolecules
931 Relevant for Microalgae Liquefaction. *Ind Eng Chem Res* 2015;54:1733-11758.
- 932 [42] Anderson EM, Stone ML, Katahira R, Reed M, Muchero W, Ramirez KJ, Beckham GT,
933 Roman-Leshkov Y. Differences in S/G ratio in natural poplar variants do not predict

- 934 catalytic depolymerization monomer yields. *Nat Commun* 2019;10:2033.
- 935 [43] Ralph J, Lapierre C, Boerjan W. Lignin structure and its engineering. *Curr Opin*
936 *Biotechnol* 2019;56:240-249.
- 937 [44] Yoo CG, Dumitrache A, Muchero W, Natzke J, Akinosho H, Li M, Sykes RW, Brown
938 SD, Davison B, Tuskan GA, Pu Y, Ragauskas AJ. Significance of Lignin S/G Ratio in
939 Biomass Recalcitrance of *Populus trichocarpa* Variants for Bioethanol Production. *ACS*
940 *Sustain Chem Eng* 2017;6:2162-2168.
- 941 [45] Wang S, Dai G, Yang H, Luo Z. Lignocellulosic biomass pyrolysis mechanism: A state-
942 of-the-art review. *Prog Energy Combust Sci* 2017;62:33-86.
- 943 [46] Chen WH, Lin BJ, Lin YY, Chu, YS, Ubando AT, Show PL, Ong HC, Chang JS, Ho SH,
944 Culaba AB, Pétrissans A, Pétrissans M. Progress in biomass torrefaction: Principles,
945 applications and challenges. *Prog Energy Combust Sci* 2021;82:100887.
- 946 [47] Tursi, A. A review on biomass: importance, chemistry, classification, and conversion.
947 *Biofuel Res J* 2019;6:962.
- 948 [48] Zheng M, Pang J, Sun R, Wang A, Zhang T. Selectivity Control for Cellulose to Diols:
949 Dancing on Eggs. *ACS Catal* 2017;7:1939-1954.
- 950 [49] Fan J, Shuttleworth PS, Gronnow M, Breeden SW, Clark JH, Macquarrie DJ, Budarin
951 VL. Influence of Density on Microwave Pyrolysis of Cellulose. *ACS Sustain Chem*
952 *Eng* 2018; 6:2916-2920.
- 953 [50] Zhou X, Li W, Mabon R, Broadbelt LJ. A mechanistic model of fast pyrolysis of
954 hemicellulose. *Energy Environ Sci* 2018;1:1240-1260.
- 955 [51] Chen Z, Reznicek WD, Wan C. Aqueous Choline Chloride: A Novel Solvent for
956 Switchgrass Fractionation and Subsequent Hemicellulose Conversion into Furfural.
957 *ACS Sustain Chem Eng* 2018;6:6910-6919.
- 958 [52] Liu X, Bouxin FP, Fan J, Budarin VL, Hu C, Clark JH. Microwave-assisted catalytic
959 depolymerization of lignin from birch sawdust to produce phenolic monomers utilizing
960 a hydrogen-free strategy. *J Hazard Mater* 2021;402:123490.
- 961 [53] Cao Y, Chen SS, Tsang DCW, Clark JH, Budarin VL, Hu C, Wu KCW, Zhang S.
962 Microwave-assisted depolymerization of various types of waste lignins over two-

- 963 dimensional CuO/BCN catalysts. *Green Chem* 2020;22:725-736.
- 964 [54] Wong SS, Shu R, Zhang J, Liu H, Yan N. Downstream processing of lignin derived
965 feedstock into end products. *Chem Soc Rev* 2020;49:5510-5560.
- 966 [55] Guo H, Zhang B, Qi Z, Li C, Ji J, Dai T, Wang A, Zhang T. Valorization of Lignin to
967 Simple Phenolic Compounds over Tungsten Carbide: Impact of Lignin Structure.
968 *ChemSusChem* 2017;10:523-532.
- 969 [56] Ragauskas AJ, Beckham GT, Bidy MJ, Chandra R, Chen F, Davis MF, Davison BH,
970 Dixon RA, Gilna P, Keller M, Langan P, Naskar AK, Saddler JN, Tschaplinski TJ,
971 Tuskan GA, Wyman CE. Lignin valorization: improving lignin processing in the
972 biorefinery. *Science* 2014;344:1246843.
- 973 [57] Bueren JBD, Héroguel F, Wegmann C, Dick GR, Luterbacher JS. Aldehyde-Assisted
974 Fractionation Enhances Lignin Valorization in Endocarp Waste Biomass. *ACS Sustain*
975 *Chem Eng* 2020;8:16737-16745.
- 976 [58] Cuevas M, Martinez Cartas ML, Sanchez S. Effect of Short-Time Hydrothermal
977 Carbonization on the Properties of Hydrochars Prepared from Olive-Fruit Endocarps.
978 *Energy Fuels* 2018;33:313-322.
- 979 [59] Poerschmann J, Weiner B, Koehler R, Kopinke FD. Hydrothermal Carbonization of
980 Glucose, Fructose, and Xylose-Identification of Organic Products with Medium
981 Molecular Masses. *ACS Sustain Chem Eng* 2017;5:6420-6428.
- 982 [60] Lu X, Ma X, Chen X. Co-hydrothermal carbonization of sewage sludge and
983 lignocellulosic biomass: Fuel properties and heavy metal transformation behaviour of
984 hydrochars. *Energy* 2021;221:119896.
- 985 [61] Li L, Wang Y, Xu J, Flora JRV, Hoque S, Berge ND. Quantifying the sensitivity of
986 feedstock properties and process conditions on hydrochar yield. *Bioresource*
987 *Technology* 2018;262:284-293.
- 988 [62] Wang X, Yun S, Fang W, Zhang C, Liang X, Lei Z, Liu Z. Layer-Stacking Activated
989 Carbon Derived from Sunflower Stalk as Electrode Materials for High-Performance
990 Supercapacitors. *ACS Sustain Chem Eng* 2018;6:11397-11407.
- 991 [63] Zhang X, Li Y, Wang M, Han L, Liu X. Effects of Hydrothermal Carbonization

- 992 Conditions on the Combustion and Kinetics of Wheat Straw Hydrochar Pellets and
993 Efficiency Improvement Analyses. *Energy Fuels* 2019;34:587-598.
- 994 [64] Wikberg H, Ohra-aho T, Pileidis F, Titirici MM, Structural and Morphological Changes
995 in Kraft Lignin during Hydrothermal Carbonization. *ACS Sustain Chem Eng*
996 2015;3:2737-2745.
- 997 [65] Deepa AK, Dhepe PL, Lignin Depolymerization into Aromatic Monomers over Solid
998 Acid Catalysts. *ACS Catal* 2014;5:365-379.
- 999 [66] Li H, Song G. Ru-Catalyzed Hydrogenolysis of Lignin: Base-Dependent Tunability of
1000 Monomeric Phenols and Mechanistic Study. *ACS Catal* 2019;9:4054-4064.
- 1001 [67] Zhang JW, Lu GP, Cai C. Self-hydrogen transfer hydrogenolysis of β -O-4 linkages in
1002 lignin catalyzed by MIL-100(Fe) supported Pd-Ni BMNPs. *Green Chem*
1003 2017;19:4538-4543.
- 1004 [68] Cao Y, Chen SS, Zhang S, Ok YS, Matsagar BM, Wu KC, Tsang DCW. Advances in
1005 lignin valorization towards bio-based chemicals and fuels: Lignin biorefinery.
1006 *Bioresour Technol* 2019;291:121878.
- 1007 [69] Cao Y, Zhang C, Tsang DCW, Fan J, Clark JH, Zhang S, Hydrothermal Liquefaction of
1008 Lignin to Aromatic Chemicals: Impact of Lignin Structure. *Ind Eng Chem Res*
1009 2020;59:16957-16969.
- 1010 [70] Correa CR, Stollovsky M, Hehr T, Rauscher Y, Rolli B, Kruse A. Influence of the
1011 Carbonization Process on Activated Carbon Properties from Lignin and Lignin-Rich
1012 Biomasses. *ACS Sustain Chem Eng* 2017;5:8222-8233.
- 1013 [71] Liu C, Li N, Peng L, Zhong W, Mao L, Yin D. Hydrothermal Carbonization of
1014 Renewable Natural Plants as Superior Metal-Free Catalysts for Aerobic Oxidative
1015 Coupling of Amines to Imines. *ACS Sustain Chem Eng* 2020; 8:11404-11412.
- 1016 [72] Mai D, Wen R, Cao W, Yuan B, Liu Y, Liu Q, Qian G. Effect of Heavy Metal (Zn) on
1017 Redox Property of Hydrochar Produced from Lignin, Cellulose, and d-Xylose. *ACS*
1018 *Sustainable Chem Eng* 2017;5:3499-3508.
- 1019 [73] Nzediegwu C, Naeth MA, Chang SX. Carbonization temperature and feedstock type
1020 interactively affect chemical, fuel, and surface properties of hydrochars. *Bioresour*

- 1021 Technol 2021;330:124976.
- 1022 [74] Zhang D, Wang F, Shen X, Yi W, Li Z, Li Y, Tian C. Comparison study on fuel
1023 properties of hydrochars produced from corn stalk and corn stalk digestate. Energy
1024 2018;165:527-536.
- 1025 [75] Gu D, Ma R, Zhou Y, Wang F, Yan K, Liu Q, Wang J. Synthesis of Nitrogen-Doped
1026 Porous Carbon Spheres with Improved Porosity toward the Electrocatalytic Oxygen
1027 Reduction. ACS Sustain Chem Eng 2017;5:11105-11116.
- 1028 [76] Wang H, Xiong F, Tan Y, Yang J, Qing Y, Chu F, Wu Y. Preparation and Formation
1029 Mechanism of Covalent-Noncovalent Forces Stabilizing Lignin Nanospheres and Their
1030 Application in Superhydrophobic and Carbon Materials. ACS Sustain Chem Eng
1031 2021;9:3811-3820.
- 1032 [77] Sangchoom W, Mokaya R. Valorization of Lignin Waste: Carbons from Hydrothermal
1033 Carbonization of Renewable Lignin as Superior Sorbents for CO₂ and Hydrogen
1034 Storage. ACS Sustain Chem Eng 2015;3:1658-1667.
- 1035 [78] Simsir H, Eltugral N, Karagoz S. Effects of Acidic and Alkaline Metal Triflates on the
1036 Hydrothermal Carbonization of Glucose and Cellulose. Energy Fuels 2019;33:7473-
1037 7479.
- 1038 [79] Wang J, Luo X, Young C, Kim J, Kaneti YV, You J, Kang YM, Yamauchi Y, Wu KCW.
1039 A Glucose-Assisted Hydrothermal Reaction for Directly Transforming Metal-Organic
1040 Frameworks into Hollow Carbonaceous Materials. Chem Mater 2018;30:4401-4408.
- 1041 [80] Zhang C, Jia C, Cao Y, Yao Y, Xie S, Zhang S, Lin H. Water-assisted selective
1042 hydrodeoxygenation of phenol to benzene over the Ru composite catalyst in the
1043 biphasic process. Green Chem 2019;21:1668-1679.
- 1044 [81] Zhang L, Wang Q, Wang B, Yang G, Lucia LA, Chen J. Hydrothermal Carbonization
1045 of Corncob Residues for Hydrochar Production. Energy Fuels 2015;29:872-876.
- 1046 [82] Keiller BG, Muhlack R, Burton RA, Eyk PJV. Biochemical Compositional Analysis
1047 and Kinetic Modeling of Hydrothermal Carbonization of Australian Saltbush. Energy
1048 Fuels 2019;33:12469-12479.
- 1049 [83] Saqib NU, Baroutian S, Sarmah AK. Physicochemical, structural and combustion

- 1050 characterization of food waste hydrochar obtained by hydrothermal carbonization.
1051 *Bioresour Technol* 2018;266:357.
- 1052 [84] Gupta D, Mahajani SM, Garg A. Investigation on hydrochar and macromolecules
1053 recovery opportunities from food waste after hydrothermal carbonization. *Sci Total*
1054 *Environ* 2020;749:142294.
- 1055 [85] Duman G, Balmuk G, Cay H, Kantarli IC, Yanik J. Comparative Evaluation of
1056 Torrefaction and Hydrothermal Carbonization: Effect on Fuel Properties and
1057 Combustion Behavior of Agricultural Wastes. *Energy Fuels* 2020;34:11175-11185.
- 1058 [86] Johnson S, Faradilla RHF, Venditti RA, Lucia L, Hakovirta M. Hydrothermal
1059 Carbonization of Nanofibrillated Cellulose: A Pioneering Model Study Demonstrating
1060 the Effect of Size on Final Material Qualities. *ACS Sustain Chem Eng* 2020;8:1823-
1061 1830.
- 1062 [87] Nunes RS, Tudino TC, Vieira LM, Mandelli D, Carvalho WA. Rational production of
1063 highly acidic sulfonated carbons from kraft lignins employing a fractionation process
1064 combined with acid-assisted hydrothermal carbonization. *Bioresour Technol*
1065 2020;303:122882.
- 1066 [88] Xu F, Chen Y, Tang M, Wang H, Deng J, Wang Y. Acid Induced Self-Assembly Strategy
1067 to Synthesize Ordered Mesoporous Carbons from Biomass. *ACS Sustain Chem Eng*
1068 2016;4:4473-4479.
- 1069 [89] Fang G, Liu C, Gao J, Dionysiou DD, Zhou D. Manipulation of persistent free radicals
1070 in biochar to activate persulfate for contaminant degradation. *Environ Sci Technol*
1071 2015;49:5645-53.
- 1072 [90] He X, Zhang T, Xue Q, Zhou Y, Wang H, Bolan NS, Jiang R, Tsang DCW. Enhanced
1073 adsorption of Cu(II) and Zn(II) from aqueous solution by polyethyleneimine modified
1074 straw hydrochar. *Sci Total Environ* 2021;778: 146116.
- 1075 [91] Zhu X, Liu Y, Qian F, Zhou C, Zhang S, Chen J. Role of Hydrochar Properties on the
1076 Porosity of Hydrochar-based Porous Carbon for Their Sustainable Application. *ACS*
1077 *Sustain Chem Eng* 2015;3:833-840.
- 1078 [92] Li F, Zimmerman AR, Hu X, Yu Z, Huang J, Gao B. One-pot synthesis and

- 1079 characterization of engineered hydrochar by hydrothermal carbonization of biomass
1080 with ZnCl₂. *Chemosphere* 2020;254:126866.
- 1081 [93] Xu Z, Zhang X, Li K, Lin H, Qian X, Sheng K. Green Synthesis of Fe-Decorated
1082 Carbon Sphere/Nanosheet Derived from Bamboo for High-Performance
1083 Supercapacitor Application. *Energy Fuels* 2020;35:827-838.
- 1084 [94] Wang L, Skjevrak G, Hustad JE, Skreiberg Ø. Investigation of Biomass Ash Sintering
1085 Characteristics and the Effect of Additives. *Energy Fuels* 2013;28:208.
- 1086 [95] Liu H, Chen Y, Yang H, Gentili FG, Söderlind U, Wang X, Zhang W, Chen H.
1087 Hydrothermal carbonization of natural microalgae containing a high ash content. *Fuel*
1088 2019;249:441.
- 1089 [96] Jung D, Zimmermann M, Kruse A. Hydrothermal Carbonization of Fructose: Growth
1090 Mechanism and Kinetic Model. *ACS Sustain Chem Eng* 2018;6:13877-13887.
- 1091 [97] Shi N, Liu Q, He X, Wang G, Chen N, Peng J, Ma L. Molecular Structure and Formation
1092 Mechanism of Hydrochar from Hydrothermal Carbonization of Carbohydrates. *Energy*
1093 *Fuels* 2019;33:9904-9915.
- 1094 [98] He Q, Yu Y, Wang J, Suo X, Liu Y. Kinetic Study of the Hydrothermal Carbonization
1095 Reaction of Glucose and Its Product Structures. *Ind Eng Chem Res* 2021;60:4552-4561.
- 1096 [99] Zhang J, An Y, Borrion A, He W, Wang N, Chen Y, Li G. Process characteristics for
1097 microwave assisted hydrothermal carbonization of cellulose. *Bioresour Technol*
1098 2018;259: 91-98.
- 1099 [100] Zhu X, Liu Y, Qian F, Lei Z, Zhang Z, Zhang S, Chen J, Ren ZJ. Demethanation Trend
1100 of Hydrochar Induced by Organic Solvent Washing and Its Influence on Hydrochar
1101 Activation. *Environ Sci Technol* 2017;51:10756.
- 1102 [101] Hao S, Zhu X, Liu Y, Qian F, Fang Z, Shi Q, Zhang S, Chen J, Ren ZJ. Production
1103 Temperature Effects on the Structure of Hydrochar-Derived Dissolved Organic Matter
1104 and Associated Toxicity. *Environ Sci Technol* 2018;52:7486.
- 1105 [102] Zhang Z, Jia B, Liu L, Zhao Y, Wu H, Qin M, Han K, Wang WA, Xi K, Zhang L, Qi G,
1106 Qu X, Kumar RV. Hollow Multihole Carbon Bowls: A Stress-Release Structure Design
1107 for High-Stability and High-Volumetric-Capacity Potassium-Ion Batteries. *ACS Nano*

- 1108 2019;13:11363-11371.
- 1109 [103] Peng L, Liang Y, Huang J, Xing L, Zheng M. Mixed-Biomass Wastes Derived
1110 Hierarchically Porous Carbons for High-Performance Electrochemical Energy Storage.
1111 ACS Sustainable Chem. Eng. 2019;7:10393-10402.
- 1112 [104] Jing S, Zhao Y, Sun R-C, Zhong L, Peng X. Facile and High-Yield Synthesis of Carbon
1113 Quantum Dots from Biomass-Derived Carbons at Mild Condition. ACS Sustain Chem
1114 Eng 2019;7:7833-7843.
- 1115 [105] Qi W, He C, Wang Q, Liu S, Yu Q, Wang W, Leksawasdi N, Wang C, Yuan Z. Carbon-
1116 Based Solid Acid Pretreatment in Corncob Saccharification: Specific Xylose
1117 Production and Efficient Enzymatic Hydrolysis. ACS Sustain Chem Eng 2018;6:3640-
1118 3648.
- 1119 [106] Lahive CW, Deuss PJ, Lancefield CS, Sun Z, Cordes DB, Young CM, Tran F, Slawin
1120 AM, Vries JGD, Kamer PC, Westwood NJ, Barta K. Advanced Model Compounds for
1121 Understanding Acid-Catalyzed Lignin Depolymerization: Identification of Renewable
1122 Aromatics and a Lignin-Derived Solvent. J Am Chem Soc 2016;138:8900-8911.
- 1123 [107] Qi S, Wang G, Sun H, Wang L, Liu Q, Ma G, Parvez AM, Si C. Using Lignin Monomer
1124 As a Novel Capping Agent for Efficient Acid-Catalyzed Depolymerization of High
1125 Molecular Weight Lignin to Improve Its Antioxidant Activity. ACS Sustain Chem Eng
1126 2020;8:9104-9114.
- 1127 [108] Wang S, Gao W, Li H, Xiao LP, Sun RC, Song G. Selective Fragmentation of
1128 Biorefinery Corncob Lignin into p-Hydroxycinnamic Esters with a Supported Zinc
1129 Molybdate Catalyst. ChemSusChem 2018;11:2114-2123.
- 1130 [109] Chen W, Zhang G, Li D, Ma S, Wang B, Jiang X. Preparation of Nitrogen-Doped Porous
1131 Carbon from Waste Polyurethane Foam by Hydrothermal Carbonization for H₂S
1132 Adsorption. Ind Eng Chem Res 2020;59:7447-7456.
- 1133 [110] Li Y, Meas A, Shan S, Yang R, Gai X, Wang H, Tsend N. Hydrochars from bamboo
1134 sawdust through acid assisted and two-stage hydrothermal carbonization for removal
1135 of two organics from aqueous solution. Bioresour Technol 2018;251:257-264.
- 1136 [111] Balou S, Babak SE, Priye A. Synergistic Effect of Nitrogen Doping and Ultra-

- 1137 Microporosity on the Performance of Biomass and Microalgae-Derived Activated
1138 Carbons for CO₂ Capture. *ACS Appl Mater Interfaces* 2020;12:42711-42722.
- 1139 [112] Zhang L, You T, Zhou T, Zhou X, Xu F. Interconnected Hierarchical Porous Carbon
1140 from Lignin-Derived Byproducts of Bioethanol Production for Ultra-High Performance
1141 Supercapacitors. *ACS Appl Mater Interfaces* 2016;8:13918-13925.
- 1142 [113] Tu W, Liu Y, Xie Z, Chen M, Ma L, Du G, Zhu M. A novel activation-hydrochar via
1143 hydrothermal carbonization and KOH activation of sewage sludge and coconut shell
1144 for biomass wastes: Preparation, characterization and adsorption properties. *J Colloid
1145 Interface Sci* 2021;593:390-407.
- 1146 [114] Zhou N, Zhang C, Cao Y, Zhan J, Fan J, Clark JH, Zhang S. Conversion of xylose into
1147 furfural over MC-SnO_x and NaCl catalysts in a biphasic system. *J. Clean Prod*
1148 2021;311:127780.
- 1149 [115] Liu J, Zhang X, Yang L, Danhassan UA, Zhang S, Yang M, Sheng K, Zhang X. Glucose
1150 isomerization catalyzed by swollen cellulose derived aluminum-hydrochar. *Sci Total
1151 Environ* 2021;777:146037.
- 1152 [116] Sharma HB, Dubey BK. Co-hydrothermal carbonization of food waste with yard waste
1153 for solid biofuel production: Hydrochar characterization and its pelletization. *Waste
1154 Manage* 2020;118:521.
- 1155 [117] Shao Y, Tan H, Shen D, Zhou Y, Jin Z, Zhou D, Lu W, Long Y. Synthesis of improved
1156 hydrochar by microwave hydrothermal carbonization of green waste. *Fuel*
1157 2020;266:117146.
- 1158 [118] Chen X, Zhang K, Xiao LP, Sun RC, Song G. Total utilization of lignin and
1159 carbohydrates in *Eucalyptus grandis*: an integrated biorefinery strategy towards
1160 phenolics, levulinic acid, and furfural. *Biotechnol Biofuels* 2020;13:2.
- 1161 [119] Zhang K, Li H, Xiao LP, Wang B, Sun RC, Song G. Sequential utilization of bamboo
1162 biomass through reductive catalytic fractionation of lignin. *Bioresour Technol*
1163 2019;285:121335.
- 1164 [120] Liu X, Li H, Xiao L-P, Sun R-C, Song G. Chemodivergent hydrogenolysis of
1165 eucalyptus lignin with Ni@ZIF-8 catalyst. *Green Chem* 2019;21:1498-1504.

- 1166 [121] Zhu Y, Liao Y, Lv W, Liu J, Song X, Chen L, Wang C, Sels BF, Ma L. Complementing
1167 Vanillin and Cellulose Production by Oxidation of Lignocellulose with Stirring Control.
1168 ACS Sustain Chem Eng 2020;8:2361-2374.
- 1169 [122] Fache M, Boutevin B, Caillol S. Vanillin Production from Lignin and Its Use as a
1170 Renewable Chemical. ACS Sustain Chem Eng 2015;4:35-46.
- 1171 [123] Qu C, Kaneko M, Kashimura K, Tanaka K, Ozawa S, Watanabe T. Direct Production
1172 of Vanillin from Wood Particles by Copper Oxide-Peroxide Reaction Promoted by
1173 Electric and Magnetic Fields of Microwaves. ACS Sustain Chem Eng 2017;5:11551-
1174 11557.
- 1175 [124] Hilgers R, Kabel MA, Vincken JP. Reactivity of p-Coumaroyl Groups in Lignin upon
1176 Laccase and Laccase/HBT Treatments. ACS Sustain Chem Eng 2020;8:8723-8731.
- 1177 [125] Erven GV, Wang J, Sun P, Waard PD, Putten JVD, Frissen GE, Gosselink RJA,
1178 Zinovyev G, Potthast A, Berkel WJHV, Kabel MA. Structural Motifs of Wheat Straw
1179 Lignin Differ in Susceptibility to Degradation by the White-Rot Fungus *Ceriporiopsis*
1180 *subvermispora*. ACS Sustain Chem Eng 2019;7:20032-20042.
- 1181 [126] Peng C, Chen Q, Guo H, Hu G, Li C, Wen J, Wang H, Zhang T, Zhao ZK, Sun R, Xie
1182 H. Effects of Extraction Methods on Structure and Valorization of Corn Stover Lignin
1183 by a Pd/C Catalyst. ChemCatChem 2017;9:1135-1143.
- 1184 [127] Ralph J, Hatfield RD, Quideau S, Helm RF, Grabber JH, Jung HJG. Pathway of p-
1185 Coumaric Acid Incorporation into Maize Lignin As Revealed by NMR. J Am Chem
1186 Soc 1994;116:9448-9456.
- 1187 [128] Timokhin VI, Regner M, Motagamwala AH, Sener C, Karlen SD, Dumesic JA, Ralph
1188 J. Production of p-Coumaric Acid from Corn GVL-Lignin. ACS Sustain Chem Eng
1189 2020;8:17427-17438.
- 1190 [129] Chaudhary R, Dhepe PL. Solid base catalyzed depolymerization of lignin into low
1191 molecular weight products. Green Chem 2017;19:778-788.
- 1192 [130] Abdelaziz OY, Ravi K, Mittermeier F, Meier S, Riisager A, Lidén G, Hultberg CP.
1193 Oxidative Depolymerization of Kraft Lignin for Microbial Conversion. ACS Sustain
1194 Chem Eng 2019;7:11640-11652.

- 1195 [131] Erdocia X, Prado R, Corcuera MÁ, Labidi J. Base catalyzed depolymerization of lignin:
1196 Influence of organosolv lignin nature. *Biomass Bioenergy* 2014;66:379-386.
- 1197 [132] Long J, Lou W, Wang L, Yin B, Li X. [C₄H₈SO₃Hmim]HSO₄ as an efficient catalyst for
1198 direct liquefaction of bagasse lignin: Decomposition properties of the inner structural
1199 units. *Chem Eng Sci* 2015;122:24-33.
- 1200 [133] Phongpreecha T, Hool NC, Stoklosa RJ, Klett AS, Foster CE, Bhalla A, Holmes D,
1201 Thies MC, Hodge DB. Predicting lignin depolymerization yields from quantifiable
1202 properties using fractionated biorefinery lignins. *Green Chem* 2017;19:5131-5143.
- 1203 [134] Shao Y, Xia Q, Dong L, Liu X, Han X, Parker SF, Cheng Y, Daemen LL, Ramirez-
1204 Cuesta AJ, Yang S, Wang Y. Selective production of arenes via direct lignin upgrading
1205 over a niobium-based catalyst. *Nat Commun* 2017;8:16104.
- 1206 [135] Dong C, Meng X, Yeung CS, Tse HY, Ragauskas AJ, Leu SY. Diol pretreatment to
1207 fractionate a reactive lignin in lignocellulosic biomass biorefineries. *Green Chem*
1208 2019;21:2788-2800.
- 1209 [136] Wang G, Liu X, Yang B, Si C, Parvez AM, Jang J, Ni Y. Using Green γ -
1210 Valerolactone/Water Solvent To Decrease Lignin Heterogeneity by Gradient
1211 Precipitation. *ACS Sustain Chem Eng* 2019;7:10112-10120.
- 1212 [137] Li YJ, Li HY, Cao XF, Sun SN, Sun RC. Understanding the Distribution and Structural
1213 Feature of Eucalyptus Lignin Isolated by γ -Valerolactone/Water/Acid System. *ACS*
1214 *Sustain Chem Eng* 2018;6:12124-12131.
- 1215 [138] Wu K, Wang W, Guo H, Yang Y, Huang Y, Li W, Li C. Engineering Co Nanoparticles
1216 Supported on Defect MoS_{2-x} for Mild Deoxygenation of Lignin-Derived Phenols to
1217 Arenes. *ACS Energy Lett* 2020;5:1330-1336.
- 1218 [139] Zhu Y, Liu J, Liao Y, Lv W, Ma L, Wang C. Degradation of Vanillin During Lignin
1219 Valorization Under Alkaline Oxidation. *Top Curr Chem* 2018;376:29.
- 1220 [140] Hafezisefat P, Lindstrom JK, Brown RC, Qi L. Non-catalytic oxidative
1221 depolymerization of lignin in perfluorodecalin to produce phenolic monomers. *Green*
1222 *Chem* 2020;22:6567-6578.
- 1223 [141] Roberts VM, Stein V, Reiner T, Lemonidou A, Li X, Lercher JA. Towards quantitative

- 1224 catalytic lignin depolymerization. *Chemistry* 2011;17:5939-48.
- 1225 [142] Renders T, Schutyser W, Van den Bosch S, Koelewijn S-F, Vangeel T, Courtin CM, Sels
1226 BF. Influence of Acidic (H₃PO₄) and Alkaline (NaOH) Additives on the Catalytic
1227 Reductive Fractionation of Lignocellulose. *ACS Catal* 2016;6:2055-2066.
- 1228 [143] Liu Y, Li C, Miao W, Tang W, Xue D, Li C, Zhang B, Xiao J, Wang A, Zhang T, Wang
1229 C, Mild Redox-Neutral Depolymerization of Lignin with a Binuclear Rh Complex in
1230 Water. *ACS Catal* 2019;9:4441-4447.
- 1231 [144] Mellmer MA, Sanpitakseree C, Demir B, Ma K, Elliott WA, Bai P, Johnson RL, Walker
1232 TW, Shanks BH, Rioux RM, Neurock M, Dumesic JA. Effects of chloride ions in acid-
1233 catalyzed biomass dehydration reactions in polar aprotic solvents. *Nat Commun*
1234 2019;10:1132.
- 1235 [145] Mellmer MA, Sener C, Gallo JM, Luterbacher JS, Alonso DM, Dumesic JA. Solvent
1236 effects in acid-catalyzed biomass conversion reactions. *Angew Chem Int Ed Engl*
1237 2014;53:11872-11875.
- 1238 [146] Xue B, Yang Y, Zhu M, Sun Y, Li X. Lewis acid-catalyzed biphasic 2-
1239 methyltetrahydrofuran/H₂O pretreatment of lignocelluloses to enhance cellulose
1240 enzymatic hydrolysis and lignin valorization. *Bioresour Technol* 2018;270:55-61.
- 1241 [147] Zhao B, Hu Y, Gao J, Zhao G, Ray MB, Xu CC. Recent Advances in Hydroliquefaction
1242 of Biomass for Bio-oil Production Using In Situ Hydrogen Donors. *Ind Eng Chem Res*
1243 2020;59:16987-17007.
- 1244 [148] Hwang KR, Choi IH, Choi HY, Han JS, Lee KH, Lee JS. Bio fuel production from
1245 crude *Jatropha* oil; addition effect of formic acid as an in-situ hydrogen source. *Fuel*
1246 2016;174:107-113.
- 1247 [149] Li Y, Cai Z, Liao M, Long J, Zhao W, Chen Y, Li X. Catalytic depolymerization of
1248 organosolv sugarcane bagasse lignin in cooperative ionic liquid pairs. *Catal Today*
1249 2017;298:168-174.
- 1250 [150] Zhai Y, Li C, Xu G, Ma Y, Liu X, Zhang Y. Depolymerization of lignin via a non-
1251 precious Ni-Fe alloy catalyst supported on activated carbon. *Green Chem*
1252 2017;19:1895-1903.

- 1253 [151] Nam DH, Taitt BJ, Choi KS. Copper-Based Catalytic Anodes To Produce 2,5-
1254 Furandicarboxylic Acid, a Biomass-Derived Alternative to Terephthalic Acid. ACS
1255 Catal 2018;8:1197-1206.
- 1256 [152] Xiao G, Montgomery JRD, Lancefield CS, Panovic I, Westwood NJ. Copper-Mediated
1257 Conversion of Complex Ethers to Esters: Enabling Biopolymer Depolymerisation
1258 under Mild Conditions. Chemistry 2020;26:12397-12402.
- 1259 [153] Mottweiler J, Puche M, Rauber C, Schmidt T, Concepcion P, Corma A, Bolm C.
1260 Copper- and Vanadium-Catalyzed Oxidative Cleavage of Lignin using Dioxygen.
1261 ChemSusChem 2015;8:2106-13.
- 1262 [154] Feng Y, Yan G, Wang T, Jia W, Zeng X, Sperry J, Sun Y, Tang X, Lei T, Lin L. Cu¹-Cu⁰
1263 bicomponent CuNPs@ZIF-8 for highly selective hydrogenation of biomass derived 5-
1264 hydroxymethylfurfural. Green Chem 2019;21:4319-4323.
- 1265 [155] Li H, Song G. Paving the Way for the Lignin Hydrogenolysis Mechanism by
1266 Deuterium-Incorporated β-O-4 Mimics. ACS Catalysis 2020;10:12229-12238.
- 1267 [156] Rahimi A, Ulbrich A, Coon JJ, Stahl SS. Formic-acid-induced depolymerization of
1268 oxidized lignin to aromatics. Nature 2014;515:249-52.
- 1269 [157] Shuai L, Amiri MT, Questell-Santiago YM, Heroguel F, Li Y, Kim H, Meilan R,
1270 Chapple C, Ralph J, Luterbacher JS. Formaldehyde stabilization facilitates lignin
1271 monomer production during biomass depolymerization. Science 2016;354:329.
- 1272 [158] Wang M, Lu J, Zhang X, Li L, Li H, Luo N, Wang F. Two-Step, Catalytic C-C Bond
1273 Oxidative Cleavage Process Converts Lignin Models and Extracts to Aromatic Acids.
1274 ACS Catal 2016;6:6086-6090.
- 1275 [159] Shuai L, Saha B. Towards high-yield lignin monomer production. Green Chem
1276 2017;19:3752-3758.
- 1277 [160] Stein TV, Hartog TD, Buendia J, Stoychev S, Mottweiler J, Bolm C, Klankermayer J,
1278 Leitner W. Ruthenium-catalyzed C-C bond cleavage in lignin model substrates. Angew
1279 Chem Int Ed Engl 2015;54:5859-63.
- 1280 [161] Dong L, Lin L, Han X, Si X, Liu X, Guo Y, Lu F, Rudić S, Parker SF, Yang S, Wang
1281 Y.k Breaking the Limit of Lignin Monomer Production via Cleavage of Interunit

- 1282 Carbon-Carbon Linkages. *Chem* 2019;5:1521-1536.
- 1283 [162] Scown CD, Baral NR, Yang M, Vora N, Huntington T. Technoeconomic analysis for
1284 biofuels and bioproducts. *Curr Opin Biotechnol* 2021;67:58.
- 1285 [163] Klein-Marcuschamer D, Simmons BA, Blanch HW. Techno-economic analysis of a
1286 lignocellulosic ethanol biorefinery with ionic liquid pre-treatment. *Biofuels Bioprod*
1287 *Biorefin* 2011;5:562.
- 1288 [164] Akbari M, Oyedun AO, Kumar A. Comparative energy and techno-economic analyses
1289 of two different configurations for hydrothermal carbonization of yard waste. *Bioresour*
1290 *Technol Rep* 2019;7:100210.
- 1291 [165] Mazumder S, Saha P, McGaughy K, Saba A, Reza MT. Technoeconomic analysis of
1292 co-hydrothermal carbonization of coal waste and food waste. *Biomass Conv Biorefin*
1293 2020, DOI:10.1007/s13399-020-00817-8 10.1007/s13399-020-00817-8.
- 1294 [166] Mahmood R, Parshetti GK, Balasubramanian R. Energy, exergy and techno-economic
1295 analyses of hydrothermal oxidation of food waste to produce hydro-char and bio-oil.
1296 *Energy* 2016;102:187.
- 1297 [167] Zeymer M, Meisel K, Clemens A, Klemm M. Technical, Economic, and Environmental
1298 Assessment of the Hydrothermal Carbonization of Green Waste. *Chem Eng Technol*
1299 2017;40:260.
- 1300 [168] Khwanjaisakun N, Amornraksa S, Simasatitkul L, Charoensuppanimit P,
1301 Assabumrungrat S. Techno-economic analysis of vanillin production from Kraft lignin:
1302 Feasibility study of lignin valorization. *Bioresour Technol* 2020;299:122559.
- 1303 [169] Funkenbusch LT, Mullins ME, Vamling L, Belkhier T, Srettiwat N, Winjobi O,
1304 Shonnard DR, Rogers TN. Technoeconomic assessment of hydrothermal liquefaction
1305 oil from lignin with catalytic upgrading for renewable fuel and chemical production.
1306 *WIREs Energy Environ* 2019;8:e319.
- 1307 [170] Xiong X, Yu IKM, Dutta S, Masek O, Tsang DCW. Valorization of humins from food
1308 waste biorefinery for synthesis of biochar-supported Lewis acid catalysts. *Sci Total*
1309 *Environ* 2021; 775:145851.

1310